

**DESIGN AND OPTIMIZATION OF PARALLEL MANIPULATORS FOR
REHABILITATION**



**A THESIS SUBMITTED TO
THE GRADUATE SCHOOL OF NATURAL AND APPLIED SCIENCES
OF
ÇANKAYA UNIVERSITY**

BY

SAMET YAVUZ

**IN PARTIAL FULFILLMENT OF THE REQUIREMENTS
FOR
THE DEGREE OF MASTER OF SCIENCE
IN
MECHANICAL ENGINEERING**

NOVEMBER 2017

Title of the Thesis: **Design and Optimization of Parallel Manipulators for Rehabilitation**

Submitted by **Samet Yavuz**

Approval of the Graduate School of Natural and Applied Sciences, Çankaya University.



Prof. Dr. Can ÇOĞUN

Director

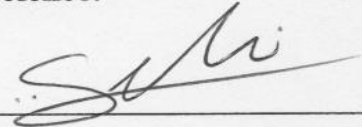
I certify that this thesis satisfies all the requirements as a thesis for the degree of Master of Science.



Prof. Dr. Sıtkı Kemal İDER

Head of Department

This is to certify that we have read this thesis and that in our opinion it is fully adequate, in scope and quality, as a thesis for the degree of Master of Science.



Asst. Prof. Dr. Özgün SELVİ

Supervisor

Examination Date: 20.11.2017

Examination Committee Members

Prof. Dr. Sıtkı Kemal İDER (Çankaya Univ.)

Asst. Prof. Dr. Özgün SELVİ (Çankaya Univ.)

Assoc. Prof. Dr. Erhan İlhan KONUKSEVEN (METU)



STATEMENT OF NON-PLAGIARISM PAGE

I hereby declare that all information in this document has been obtained and presented in accordance with academic rules and ethical conduct. I also declare that, as required by these rules and conduct, I have fully cited and referenced all material and results that are not original to this work.

Name, Last Name : Samet YAVUZ

Signature : 

Date : 29.11.2017

ABSTRACT

DESIGN AND OPTIMIZATION OF PARALLEL MANIPULATORS FOR REHABILITATION

YAVUZ, Samet

M. Sc., Department of Mechanical Engineering

Supervisor: Asst. Prof. Dr. Özgün SELVİ

November 2017, 63 pages

In this thesis, a novel over-constrained parallel manipulator for arm rehabilitation is introduced. This manipulator is a planar-spherical parallel manipulator with five degrees of freedom and four legs for rehabilitation of forearm (wrist, elbow and shoulder joints). First of all, the desired motions are specified. Then, manipulator geometry is proposed to ensure these motions. Inverse kinematic solutions are performed for describing the motion of actuators. Jacobian analysis is done to define singularity conditions and to obtain force-torque relation between user and the manipulator. The manipulator optimized dimensionally by using Firefly Algorithm to provide motions in workspace boundaries without any singularity condition. Obtained dimensional parameters are tested and whole workspace is scanned with several simulations to ensure whether the manipulator provide the given motions in specified workspace boundaries.

Keywords: Rehabilitations robotics, over-constrained manipulators, kinematic analysis, dimensional optimization

ÖZ

REHABİLİTASYON AMAÇLI PARALEL EYLEYİCİLERİN TASARIMI VE EN İYİLEMESİ

YAVUZ, Samet

Yüksek Lisans, Makine Mühendisliği Ana Bilim Dalı

Tez Yöneticisi: Yrd. Doç. Dr. Özgün SELVİ

Kasım 2017, 63 sayfa

Bu tezde kol rehabilitasyonunda kullanmak amacıyla yeni bir aşırı-tanımlı paralel eyleyici tanıtılmıştır. Bu eyleyici beş serbestlik derecesine ve dört bacağa sahip düzlemsel-küresel bir paralel eyleyicidir. Öncelikle, eyleyicinin yapması istenen hareketler tanımlanmıştır. Daha sonra bu hareketleri sağlayacak eyleyici geometrisi belirlenmiştir. Ters kinematik çözümler eyleticilerin davranışlarını saptamak amacıyla gerçekleştirilmiştir. Tekilsellik koşullarını saptamak ve ortam ile eyleticiler arasında kuvvet-tork dengesini kurabilmek için Jakobian analizi gerçekleştirilmiştir. Ateş Böceği Algoritması kullanılarak, eyleyici boyutsal olarak eniyilenmiştir. Elde edilen boyutsal parametreler çalışma alanı sınırları içerisinde çeşitli testler benzetim yapılarak gerçekleştirilmiştir.

Anahtar Kelimeler: Rehabilitasyon robotları, aşırı-kapalı eyleyiciler, kinematik analiz, boyutsal eniyileme

ACKNOWLEDGEMENTS

I would like to express my sincere gratitude to Asst. Prof. Dr. Özgün SELVİ for his supervision, guidance, suggestions, and encouragement throughout the development of this thesis.

I thank my family for their valuable support and patience.



TABLE OF CONTENTS

STATEMENT OF NON PLAGARISM	iii
ABSTRACT	iv
ÖZ	v
ACKNOWLEDGEMENTS	vi
TABLE OF CONTENTS	vii
LIST OF FIGURES	ix
LIST OF TABLES	x

CHAPTERS

1. INTRODUCTION	1
1.1. Types of Manipulators	1
1.1.1. Serial Manipulators	1
1.1.2. Parallel Manipulators	3
1.1.3. Hybrid Manipulators	4
1.2. Applications of Parallel Manipulators	4
1.3. Literature Survey on Rehabilitation and Rehabilitation Applications	7
1.4. Design and Optimization of Parallel Manipulators for Rehabilitation	11
2. STRUCTURAL ANALYSIS OF THE MANIPULATOR	13
2.1. Manipulator Geometry	14
2.2. Workspace Specification of the Manipulator	18
3. KINEMATIC ANALYSIS OF THE MANIPULATOR	19
3.1. Inverse Kinematic Solutions for Upper Part	20
3.2. Inverse Kinematic Solutions for Lower Part	22
4. JACOBIAN ANALYSIS OF THE MANIPULATOR	25
4.1. Jacobian Analysis of the Upper Part	26
4.2. Jacobian Analysis of the Lower Part	27
5. DIMENSIONAL OPTIMIZATION OF THE MANIPULATOR	29

5.1. Optimization Method (Firefly Algorithm)	32
5.2. Optimization of Upper Part.....	34
5.3. Optimization of Lower Part	35
6. TEST OF OPTIMIZED PARAMETERS WITH DESIRED MOVEMENTS INTO WORK SPACE	38
6.1. Simulations on Upper Part.....	38
6.2. Simulations on Lower Part	45
6.3. Simulations on Whole Manipulator	49
7. FORCE ANALYSIS OF THE MANIPULATOR	60
8. CONCLUSION	62
REFERENCES	R1
Appendix A: Simmechanics Models of Manipulator	A1
Appendix B: Several Views of Obtained Manipulator	A3

LIST OF TABLES

TABLES

Table 1	Types of manipulators.....	2
Table 2	Literature survey on rehabilitation robotics.....	8
Table 3	Workspace boundaries for human wrist.....	18
Table 4	Selected Firefly Algorithm parameters for spherical part.....	34
Table 5	Optimized dimensional parameters for spherical part.....	35
Table 6	Selected Firefly Algorithm parameters for planar part.....	35
Table 7	Optimized dimensional parameters for planar part.....	36
Table 8	Simulations on spherical part.....	39
Table 9	Simulations on planar part.....	46
Table 10	Simulations on whole manipulator.....	49

LIST OF FIGURES

FIGURES

Figure 1	A Serial manipulator.....	2
Figure 2	A Parallel manipulator.....	3
Figure 3	A Hybrid manipulator.....	4
Figure 4	Parallel manipulators for simulation.....	5
Figure 4 (a)	Stewart platform.....	5
Figure 4 (b)	Octahedral hexapod parallel manipulator.....	5
Figure 4 (c)	3 DOFs spherical manipulator.....	5
Figure 5	Industrial applications of parallel manipulators.....	6
Figure 5 (a)	Automatic spray painting manipulator.....	6
Figure 5 (b)	Universal tyre testing machine.....	6
Figure 5 (c)	Delta robot.....	6
Figure 5 (d)	A cable-driven parallel manipulator.....	6
Figure 6	Medical applications of parallel manipulators.....	6
Figure 6 (a)	Brain surgery bot.....	6
Figure 6 (b)	Knee surgery bot.....	6
Figure 6 (c)	Delta robot application for brain scanning.....	6
Figure 7	Determination of the movements.....	13
Figure 8	Movements of a sphere in a 5 DOFs sub-space.....	14
Figure 9	Parts of the manipulator.....	15
Figure 9 (a)	Proposed manipulator.....	15
Figure 9 (b)	Proposed manipulator with imaginary links.....	15
Figure 9 (c)	Upper part of proposed manipulator with imaginary links.....	15
Figure 9 (d)	Lower part of proposed manipulator with imaginary links.....	15
Figure 10	Human wrist movements.....	16

Figure 11	General form of a manipulator with 3 closed loops and 20 revolute joints.....	17
Figure 12	Loops of the manipulator.....	17
Figure 13 (a)	Orientation of the end-effector.....	19
Figure 13 (b)	Spherical part of the manipulator.....	19
Figure 14 (a)	First leg of the planar part.....	20
Figure 14 (b)	Fourth leg of the planar part.....	20
Figure 15	Graphical representation of function generation.....	30
Figure 16	Fourbar for motion generation.....	30
Figure 17	Optimized and assembled manipulator.....	37
Figure 18 (a)	Set 1, simulation A.....	39
Figure 18 (b)	Set 1, simulation B.....	41
Figure 18 (c)	Set 1, simulation C.....	41
Figure 18 (d)	Set 1, simulation D.....	41
Figure 18 (e)	Set 2, simulation A.....	41
Figure 18 (f)	Set 2, simulation B.....	42
Figure 18 (g)	Set 2, simulation C.....	42
Figure 18 (h)	Set 2, simulation D.....	43
Figure 18 (i)	Set 3, simulation A.....	43
Figure 18 (j)	Set 3, simulation B.....	44
Figure 18 (k)	Set 3, simulation C.....	44
Figure 18 (l)	Set 3, simulation D.....	45
Figure 19 (a)	Test results for planar part optimization (Set1).....	47
Figure 19 (b)	Test results for planar part optimization (Set 2).....	47
Figure 19 (c)	Test results for planar part optimization (Set 3).....	48
Figure 19 (d)	Test results for planar part optimization (Set 4).....	48
Figure 19 (e)	Test results for planar part optimization (Set 5).....	49
Figure 20 (a)	Test results for whole part manipulator (Set 1).....	52

Figure 20 (b)	Test results for whole part manipulator (Set 2).....	53
Figure 20 (c)	Test results for whole part manipulator (Set 3).....	53
Figure 20 (d)	Test results for whole part manipulator (Set 4).....	54
Figure 20 (e)	Test results for whole part manipulator (Set 5).....	54
Figure 20 (f)	Test results for whole part manipulator (Set 6).....	55
Figure 20 (g)	Test results for whole part manipulator (Set 7).....	55
Figure 20 (h)	Test results for whole part manipulator (Set 8).....	56
Figure 20 (i)	Test results for whole part manipulator (Set 9).....	56
Figure 20 (j)	Test results for whole part manipulator (Set 10).....	57
Figure 20 (k)	Test results for whole part manipulator (Set 11).....	57
Figure 20 (l)	Test results for whole part manipulator (Set 12).....	58
Figure 20 (m)	Test results for whole part manipulator (Set 13).....	58
Figure 20 (n)	Test results for whole part manipulator (Set 14).....	59
Figure 20 (o)	Test results for whole part manipulator (Set 15).....	59
Figure 21	Simmechanics model of spherical part.....	A1
Figure 22	Simmechanics model of planar part.....	A1
Figure 23	Simmechanics model of whole manipulator.....	A2
Figure 24	PID control model of any active joint.....	A2
Figure 25	Top view of the manipulator.....	A3
Figure 26	Front view of the manipulator.....	A4
Figure 27	A detailed view of spherical part.....	A4

1. INTRODUCTION

1.1. Types of Manipulators

Manipulators are devices designed to perform special tasks such as carrying objects, pick and place applications, welding, painting, assembling, entertainment, medical cure, surgery etc. Basic classification for manipulators can be lay out according to their DOFs, kinematic structures, actuator types, workspace geometry and motion characteristics [1].

Normally, 3 dimensional movements require 6 DOFs. If a manipulator can freely move towards and rotate in anyway in 3 dimensional space, we can call this type of a manipulator as general purpose manipulator. If this manipulator has more than 6 DOFs it's called redundant and with less than 6 DOFs it's called deficient manipulator. Manipulators also defined by types of actuator used to drive them such as electric, hydraulic and pneumatic. A volume scanned by an end-effector of a manipulator called workspace. Manipulators can be classified with shape of their workspace too. This classification can be made by taking into consideration the used joint types. Three perpendicular prismatic joints give Cartesian workspace. If we replace one prismatic joint with a revolute joint, then it's workspace geometry will be a cylinder. If replace this joint with a spherical joint instead of a revolute one, this time it's workspace will be a sphere. Motion type is one of the classification subject for manipulators. If a manipulator operates in a plane, we can call it as a planar manipulator. If this manipulator consists of only spherical links, it is a spherical manipulator. If this manipulator both performs planar and spherical motion this manipulator is a spatial manipulator. The most well-known classification for manipulator is according to their kinematic structures. In this classification, how manipulators connected to the ground is taken into consideration. We can examine manipulators in kinematic structure topics as serial, parallel and hybrid manipulators. In this thesis, types of proposed manipulator in listed categories is given Table 1. below.

1.1.1. Serial Manipulators

Serial manipulators have joints which are attached end to end (Figure 1). Because of their structural resemblance to the human arm, they also called as robotic arms. Generally, they consist of revolute and prismatic joints. There must be an actuator attached at each joints. Because of actuators are attached to make a chain each actuator

supports the movement of the next actuator. They mounted ground at a single point so their free ends can scan a large workspace. It is easy to solve their direct kinematic equations. In addition, they have high dexterity.

Table 1. Types of manipulators

DOFs	6 DOFs	Redundant	Deficient
Actuators	Electric	Hydraulic	Pneumatic
Workspace	Cartesian	Cylindrical	Spherical
Motion	Planar	Spherical	Spatial
Structure	Serial	Parallel	Hybrid

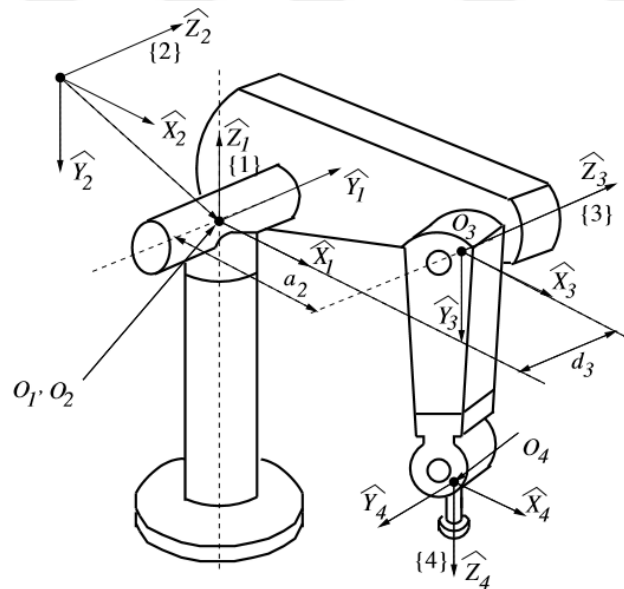


Figure 1. A Serial manipulator [2]

Compared to these advantages, joint failures of each actuator are added and effect the end-effector as a sum. Their load carrying capacity is low with respect to their weight and they have high inertia. Also, it is hard to solve their inverse kinematic equations.

1.1.2. Parallel Manipulators

Parallel manipulators have moving platforms which are connected to the ground with several chains (Figure 2). Their chains are short and simple. This causes to gain extra rigidity to the parallel manipulators. Failures do not affect the moving platform as sum like serial manipulators. There is no need to carry the load of the actuators because they are attached to the ground. Fast systems with lightweight links and small actuators or systems with high load carry capacity can be designed.

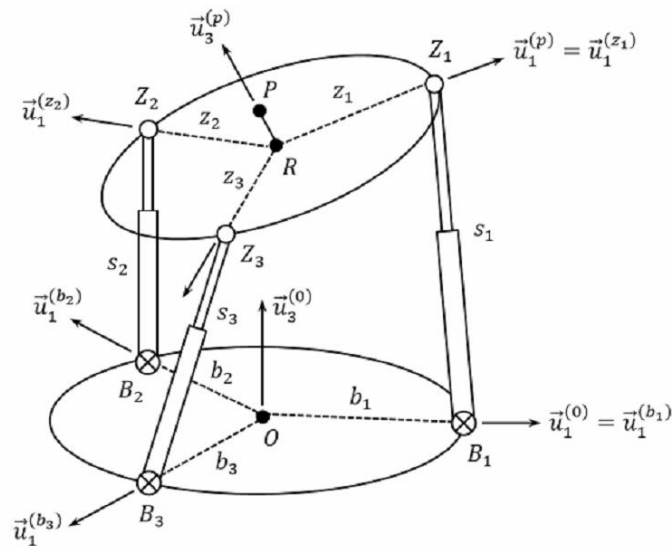


Figure 2. A Parallel manipulator [3]

Parallel manipulators have limited workspaces. Because of singularity, either they gain one or more DOF and lose their rigidity or lose one or more DOF and gain infinite rigidity. It is hard to solve their direct kinematic equations, so it is reasonable to determine a workspace and search the dimensional parameters to fulfill this workspace. Dimensional optimization is required to avoid singularity conditions. At this point optimization algorithms should be used.

1.1.3. Hybrid Manipulators

They consist of parallel and serial manipulators combination. Hybrid manipulators have both open and closed chains. Hybrid manipulators can be defined as modular manipulators. This means that hybrid manipulators can be widened by adding extra modules. Each module has hemispherical workspace and this situation cause rising of dexterous symmetrical workspace [4]. They could contain advantages and disadvantages of both parallel and serial manipulators (Figure 3).

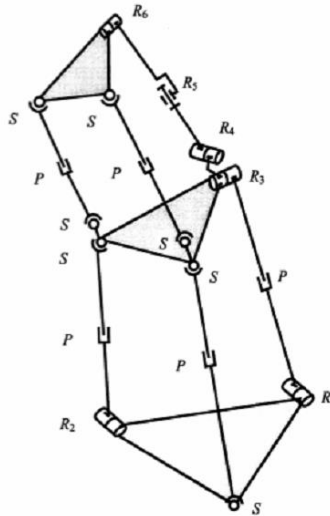


Figure 3. A Hybrid manipulator [4]

1.2. Applications of Parallel Manipulators

Parallel manipulators can find various application areas such as simulation, industrial, medical, rehabilitation etc. As a simulation manipulator, first and the most popular parallel manipulator was proposed by Stewart in 1965 [5] (Figure 4.a). This manipulator has six pods, six spherical and universal joints and six DOFs. After that, Klaus Capper patented an octahedral hexapod parallel manipulator to be used as simulation manipulator (Figure 4.b). 3 DOFs spherical parallel manipulator was used as a camera orientation device and a simulator (Figure 4.c).

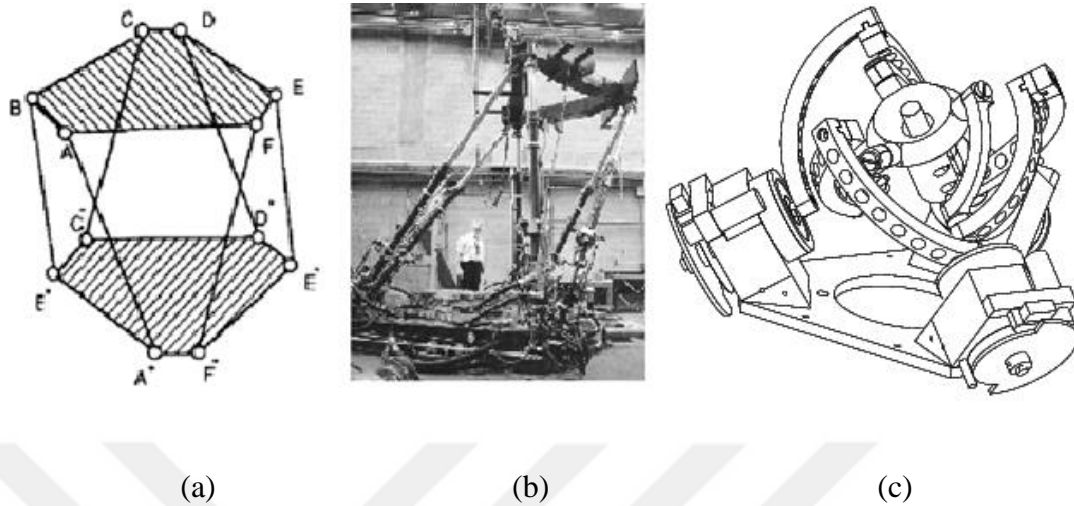


Figure 4. Parallel manipulators for simulation, (a) Stewart platform [5], (b) Octahedral hexapod parallel manipulator [6], (c) 3 DOFs spherical manipulator [45]

In industrial area, one of the first designs by William L. Pollard is a 5 DOFs which has 3 DOFs for positioning and 2 DOFs orientation, novel parallel automatic spray painting manipulator in 1942 [7] (Figure 5.a). In 1954, Dr. Eric Gough proposed a 6 DOFs parallel manipulator for universal tyre testing machine [8] (Figure 5.b). Stewart platform which was mentioned above is used for underground excavation device in milling machines. Parallel cube manipulators are used in places which requires micro motion, in remote center compliance devices, for assembling processes. Hexapods are one another type of industrial parallel manipulators and they are used in manufacturing, inspection and research areas. Delta robots are used in industrial areas such as packaging, assembly of electrical components, pick and place applications so on (Figure 5.c). One other type of parallel manipulator is cable-driven ones and their application areas can be listed as; cutting, excavating and grading, shaping and finishing, lifting and positioning [9] (Figure 5.d). Main applications areas for parallel manipulators can be listed as; welding, grinding, cutting, inspection, material handling, pipe fitting, oil-well firefighting, ship building, bridge construction, air craft maintenance, ship-to-ship cargo handling, steel erection etc [9].

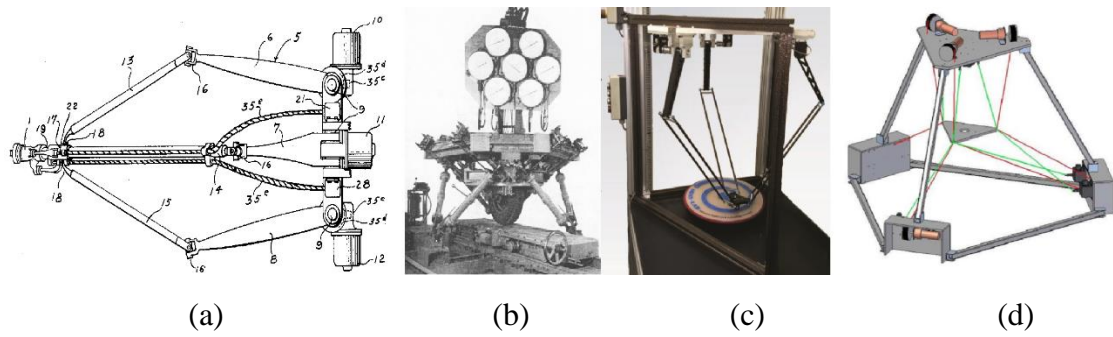


Figure 5. Industrial applications of parallel manipulator, (a) automatic spray painting manipulator [7], (b) universal tyre testing machine [8], (c) delta robot [5], (d) a cable-driven parallel manipulator [9]

Medical application is one of the application areas of the parallel manipulators. Having better precision and stiffness than serial manipulators make parallel manipulators popular in medical applications such as certain aneurysms, brain tumor, cervical spine problems, body joint surgery operations. Medical applications of parallel manipulators can be shown in Figure 6 below.

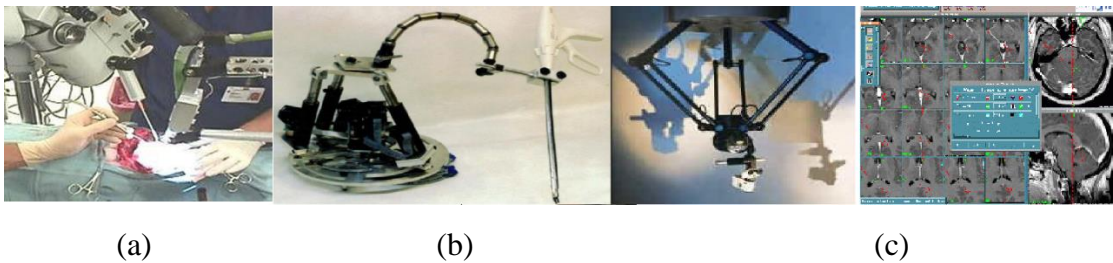


Figure 6. Medical applications of parallel manipulators [10], (a) Brain surgery bot, (b) knee surgery bot, (c) delta robot application for brain scanning

1.3. Literature Survey on Rehabilitation Applications in Robotics

The meaning of rehabilitation is recovery of injured body parts. Rehabilitation can be applied to tissues which have activity limitations and muscle-bone injuries by using heat, electrical current, human assist or robotic systems. These kind of disabilities could come from birth and they could be happened later as well. Rehabilitation is a process includes two phases diagnosis and therapy. In addition to these phases, patients should be supported psychologically. Rehabilitation can be applied following situations such as; neurologic injuries, paralysis, orthopedic problems, shoulder-elbow-wrist joint variables, tension on shoulder-back muscles, muscle spasms, backache, spinal disc herniation, neck arthritis, position disorders, kyphosis, hip-knee injuries, bone losses, limitation of movement etc.

The most common application of physiotherapy is electrotherapy. It is expected physical, chemical or mechanical effect on the application part of human body with applied electrical current. In this situation, it is seemed real time movements of muscles are more useful. Also, there is always risk of burn because of electrical current.

Physiotherapy is a branch that requires much repetitions to be effective and has been practiced for a long time period with physiotherapists' own efforts and direct interventions. In today's world, by the usage of rehabilitation robots and mechanisms, the rehabilitation motions are performed more effectively [46]. There aren't many robots for the orthopedic treatment of the upper extremity on the market, the ones that are for this treatment usually have not considered implementing the daily living activities applications and can't control multiple joints.

The upper extremity is frequently exposed to injuries because it is a region where most of the activities of daily living take place. As it is an anatomically complex structure, the movement systems used in rehabilitation are more limited than the lower extremities. With the prolongation of human life and the increase of the population over the age of 65 on the world, the likelihood of physical health problems has increased [11]. Physiotherapy and rehabilitation aim to increase the life quality by disposing or shortening physical disabilities and to reach maximum independence in daily life activities. For a long time, rehabilitation movements have been carried out by physiotherapists' own power and direct intervention, and today more effective and controlled methods have emerged in the world. The use of rehabilitation robots is an area where people can perform daily living activities in the home or business environment [12]. A large number of robots have been developed for upper extremity rehabilitation because of this region (the region covering shoulder to hand) is a vital region which enables people to perform their daily life activities. The functions of the developed robots vary, and the mechanism used in the development of these robots greatly influence the robustness, workspace and precision of these robots.

Shoulder, elbow and wrist injuries are frequent problems on the upper extremity. In particular, bone fractures, muscle tears, ligament injuries and joint capsule problems of these three joints are frequently encountered injuries. Conservative or surgical treatment approaches are used in these injuries. Physiotherapy and rehabilitation practices have an important place in both treatment approaches. In recent years, static treatment methods have now left their places to more dynamic approaches. With the exercise applied considering the level of healing of the affected region, it is possible to avoid the negative effects of immobilization and stimulate tissue healing. In rehabilitation, exercises are applied as passive, active-assisted, active-resisting. Passive exercises allow movement of the limbs without allowing the muscle contract. Passive exercises are frequently preferred after orthopedic injuries and in the early postoperative periods. In the following periods, active assisted exercises are performed to enable the active movements. Active exercises start with the patient's use of their muscular strength and are complemented by movement against the resisting systems for muscle strengthening. Although there are many rehabilitation robots operating in a single joint, the number of robots operating multiple joints at the same time for orthopedic treatment is very small. Studies on rehabilitation robotic can be seen in Table 2.

Table 2. Literature survey on rehabilitation robotics

<i>Manipulator</i>	<i>Focus Area</i>	<i>Kinematics</i>
Parallel Shoulder Mechanism	Human Arm (shoulder movements) High force-low mass robotic arm exoskeleton	Parallel structure 2 RRPS 3 DOF
A Cable Driven Upper Arm Exoskeleton for Upper Extremity Rehabilitation	Shoulder to forearm	Parallel structure 5 DOF

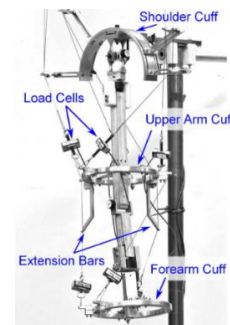
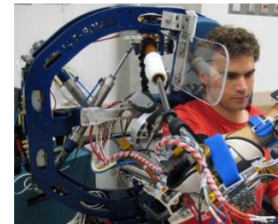
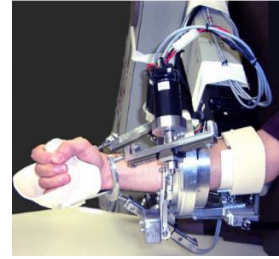


Table 2. continue

The RiceWrist: A Distal Upper Extremity Rehabilitation Robot for Stroke Therapy

From forearm to wrist

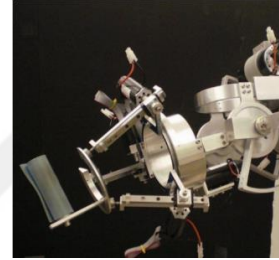
Hybrid structure
3 RPS
4 DOF



Distal Arm Exoskeleton for Stroke and Spinal Cord Injury Rehabilitation

From forearm to wrist

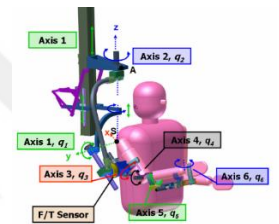
Hybrid Structure
3 RPS
5 DOF



ARMin – Exoskeleton for Arm Therapy in Stroke Patients

Human arm (fitting to its range of motion)

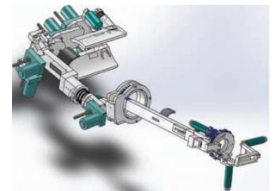
Serial Structure
6 DOF



A Bioinspired 10 DOF Wearable Powered Arm Exoskeleton for Rehabilitation

Human Arm (Shoulder girdle to wrist)

Serial Structure
10 DOF



A Haptic Knob for Rehabilitation of Hand Function

Human Hand (opening/closing of the hand)

2 DOF

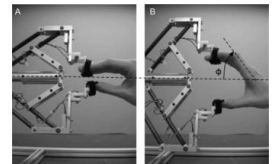
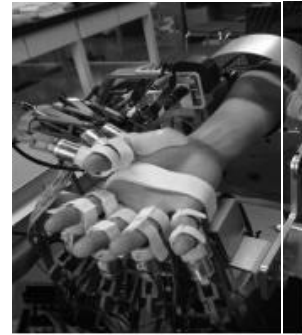


Table 2. continue

Hand-Assist Robot with Multi-Degree-of-Freedom for Rehabilitation Therapy

Human Hand (wrist and fingers)

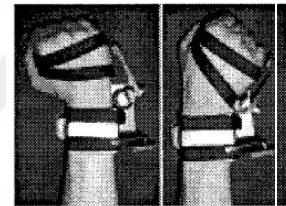
18 DOFs Serial Robot



A Robot for Wrist Rehabilitation

Human Wrist

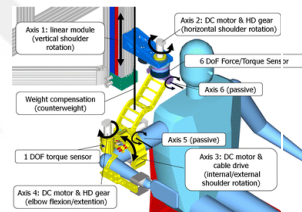
1 DOF



ARMin: a robot for patient-cooperative arm therapy

Human Arm (Shoulder, Elbow, Wrist)

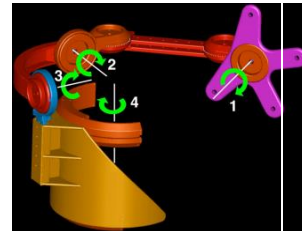
4 Active, 2 Passive DoF



Arm Exoskeleton with Scapular Motion for Shoulder Rehabilitation

Shoulder

5 DoF



Klein, Spencer et. al. [13] presented robotic-arm exoskeleton that uses a parallel mechanism to help naturalistic shoulder movements. They optimized the exoskeleton's torque capabilities by the modification of the key geometric design parameters. Mao, Agrawal [14] proposed a 5 DoF cable-driven upper arm exoskeleton, with control of force. They selected light weight cables instead of rigid links to overcome the same problems of conventional robotic rehabilitation devices such as bulkiness, heaviness and disability of the providing joint level rehabilitation. O' Malley, et. al. [15] designed

a 4 DoF upper extremity rehabilitation robot which can allow variability in methods of interference between the patient and the manipulator sort as passive, triggered and active constrained modes. Pehlivan, et.al. [16] designed a 5 DoF robot named MAHI Exo II which enables flexion-extension, and radial-ulnar deviation for the rehabilitation of upper stroke, spinal cord injury, or other brain injuries. Nef, Mihelj et.al. [16] presented an exoskeleton named ARMin which can work in different therapy modes: passive mobilization, game therapy and task-oriented training. Carignan et.al. [18] examined a 5 DoF arm exoskeleton for treating shoulder pathology. Lamercy, Dovat et.al. [18] designed a robot to train opening/closing of human hand. The design can be adaptable to various hand sizes and both hands; right and left. Kawasaki et.al. [20] designed a hand rehabilitation robot with 18 DoF uses “self-motion control” which provides patients to exercise alone with the help of their healthy hands. Williams et.al. [21] outlined the mechanical design of a robot for wrist rehabilitation. Manna [22] developed a wearable exoskeleton for human arm with 10 DoF. They focused in their research on the motion human shoulder griddle.

1.4. Design and Optimization of Parallel Manipulators for Rehabilitation

The purpose of this thesis is to improve the orthopedic treatment of patients with shoulder, elbow and wrist problems by designing a device that increase the efficiency of the treatment and help the patients adapting faster to daily living activities. Since over-constrained mechanisms are suitable for the subspace between the shoulder, elbow and the wrist, an over-constrained manipulator is suggested. The parallel mechanisms which work in subspaces are named as over-constrained mechanisms, compared to spatial mechanisms, the over-constrained mechanisms require less connectors and joints [23]. These mechanisms can be used for special cases since the system has a specified spatial boundary and are more efficient materially and in terms of application. In this project an over-constrained manipulator has been selected for the shoulder, elbow and wrist rehabilitation because of the above mentioned specifications and that there is a fitting over-constrained manipulator for the shoulder-elbow-wrist subspace. As an outcome of literature survey, rehabilitation robots using over-constrained manipulators have not been sighted. With the specified boundaries of over-constrained manipulator, a more reliable and sturdy structure will be achieved and because it is a parallel structure, compared to serial mechanism counterparts, the arm movements will be handled with more precision, power and speed. The proposed system in this thesis is proposed enable patients to adapt daily life easier. The over-constrained manipulator chosen for shoulder-elbow-wrist subspace has one-to-one correspondence thus leading to advantageous dynamics, control and usage. Aludami H. and Selvi Ö. [10] proposed an over-constrained parallel manipulator and done its

kinematic analysis. After that, Yılmaz K. and Selvi Ö. [24] made workspace analysis of the same manipulator.

In this thesis, chapter 2 lays out the geometry of the manipulator that works in a 5 dimensional space to make rehabilitation movements for shoulder-elbow-wrist joint (upper extremity). Also in this chapter, workspace boundaries are obtained to operate the manipulator in. In chapter 3, kinematic analysis of the manipulator is done. Active joint rates of the manipulator are obtained according to the orientation and position of the platform in desired workspace. In chapter 4, Jacobian analysis of the manipulator is performed. Singularity conditions of the manipulator are examined. Besides, condition number of the manipulator is calculated. In chapter 5, dimensional parameters of the manipulator are optimized to fulfill the desired workspace. Principles of the Firefly algorithm are mentioned and, constraints and objective functions of the algorithm are given. Obtained dimensional parameters presented in this chapter. In chapter 6, dimensional parameters are tested whether rotations manipulator fulfills the desired workspace and occurs any singularity. In chapter 7, force analysis of the manipulator is proposed.

2. STRUCTURAL ANALYSIS OF THE MANIPULATOR

When literature is examined for rehabilitation robotics, one could see that there are mostly serial manipulators for human wrist, elbow, shoulder or full arm rehabilitation. In this thesis, it is decided to design a manipulator which will assist patients to do both planar and spherical motions with their arms. In this regard, a manipulator is designed to combine motions for 3 DOFs rotation (wrist joint movements) and 2 DOFs translation in a plane (Figure 7).

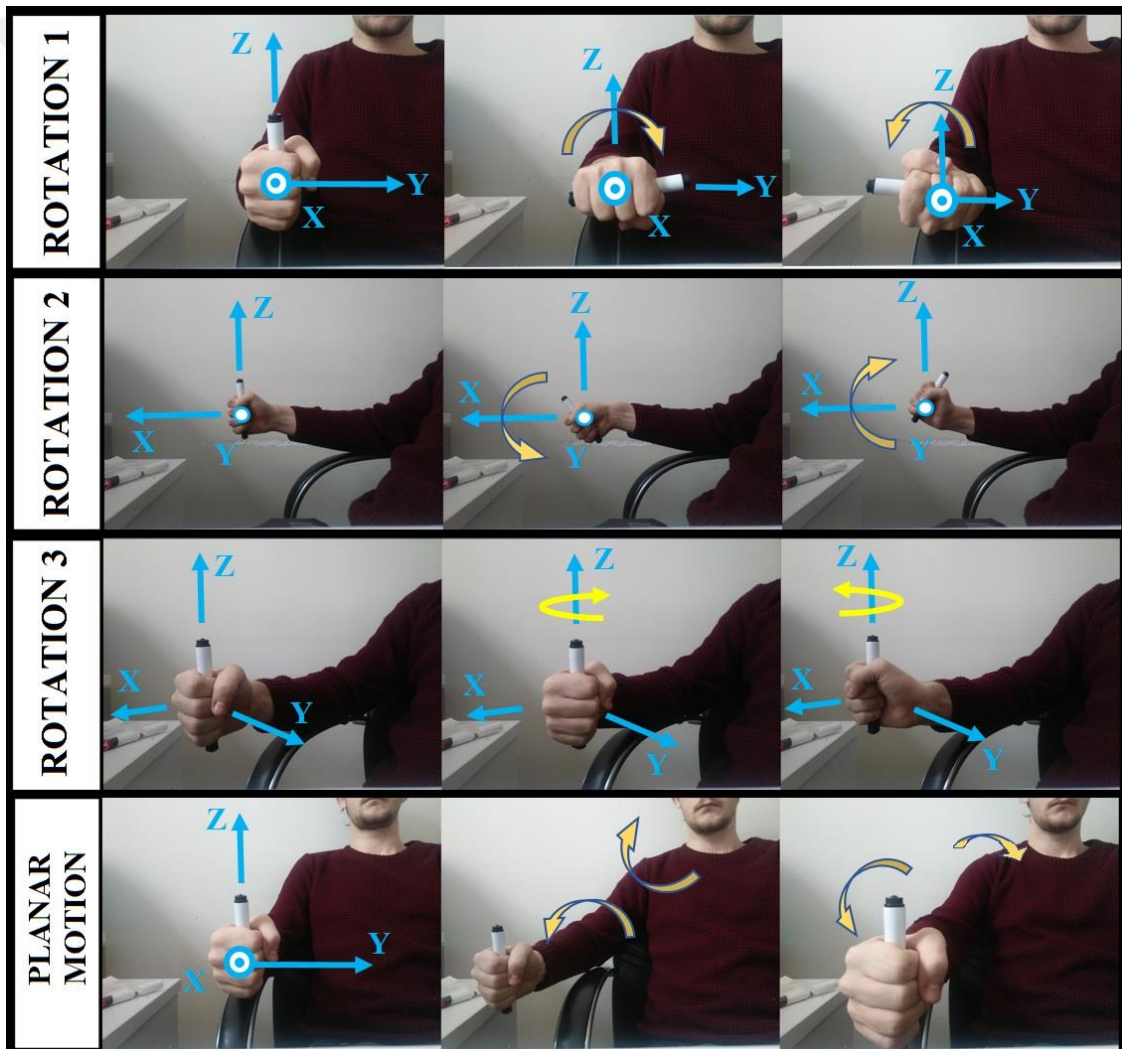


Figure 7. Determination of the movements

The mobility of the manipulator should be 5 because of 5 independent movements are defined in this study. This movement can be described with a sphere moving on a plane which can perform 3 rotations around 3 different axes and 2 translations on 2 different axes (Figure 8). When parallel manipulators compared to serial manipulators, it is known that parallel ones have several advantages such as rigidity, high load capacity etc. We can compensate 5 DOFs movements for a parallel manipulator with 3, 4 or 5 legs. With 3 legs, we need to attach two actuators on the two different legs. This configuration has a disadvantage for control of the manipulator. With 5 legs, we will have extra joints compared to the 3 or 4 legs which causes extra energy losses. So, 4 legs configuration seems best for this manipulator.

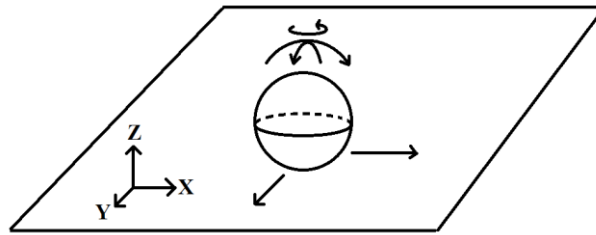


Figure 8. Movements of a sphere in a 5 DoFs sub-space

2.1. Manipulator Geometry

Designed manipulator is shown in figure 9.a below. To obtain required hand and wrist movements and to solve inverse kinematic equations, the system is divided into two sub-systems named upper and lower with using three imaginary links and joints in both two sub-systems (figure 9.b, figure 9.c and figure 9.d). All joint axes on the spherical part are intersecting at a common point P. Also, joint axes of the four imaginary links on the upper part (figure 9.d) are intersecting at the point P as well. Here spherical part will provide the 3 rotational motion of the human wrist around x, y and z axes. It is assumed that, Wrist joint does;

- pronation-supination movements about x axis
- radial-ulnar deviations about y axis
- flexion-extension movements about z axis (figure 10).

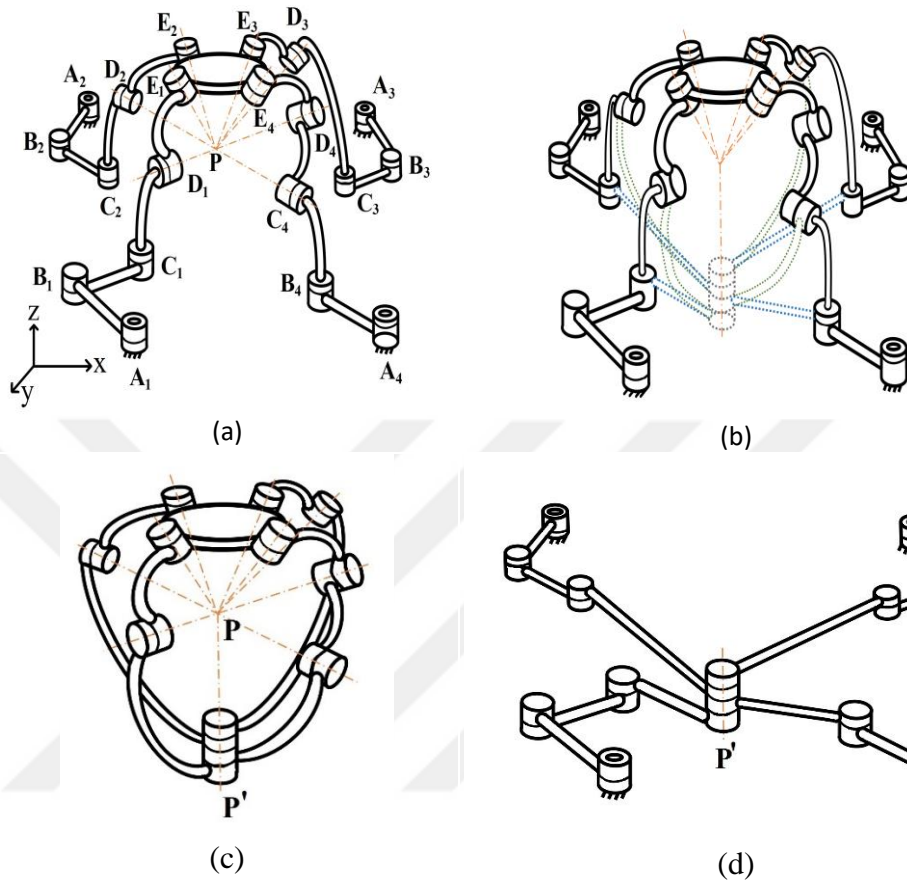


Figure 9. Parts of the manipulator (a) proposed manipulator, (b) proposed manipulator with imaginary links, (c) upper part of proposed manipulator with imaginary links, (d) lower part of proposed manipulator with imaginary links

Lower part will provide x-y plane movements of arm. All links on the lower part are in flat shape and have two joints at both ends. Their joint axes are both parallel each other and z axis of the reference coordinate system. One joint axes of the four imaginary links on the lower part (c_1 , c_2 and c_3 for first three legs and b_4 for fourth leg) are intersecting at the point P' . Point P' is the x-y plane trajectory of point P (figure 9.a).

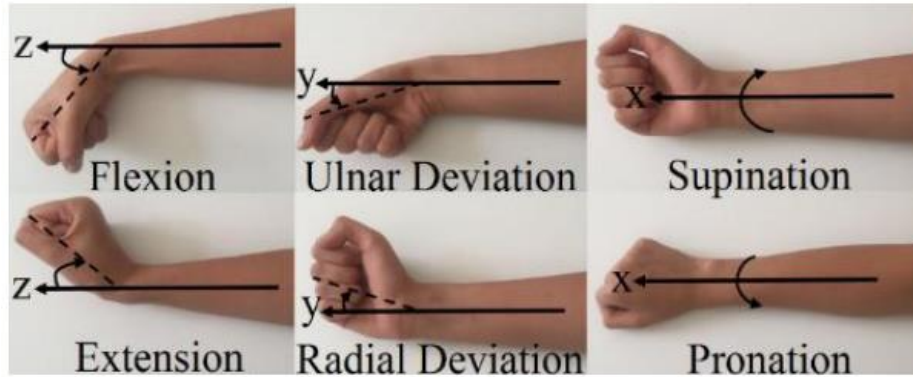


Figure 10. Human wrist movements

In addition to these properties one should noticed that, this manipulator is an asymmetrical parallel manipulator. When we compare our manipulator with symmetry conditions [1];

- Symmetrical manipulators have equal DOFs with number of limbs. Here, our manipulator has 4 limbs with 5 DOFs, so first condition is not satisfied.
- Type and number of joints in all limbs should be arranged in an identical pattern. In proposed manipulator, we have 5 revolute joints at each limb. This condition is satisfied with our manipulator.
- The number and location of all actuated in symmetrical manipulators should be the same in all limbs. As mentioned all actuator in our manipulator located at the ground plane but leg 4 have one more actuator than other 3 legs. Third condition is also not satisfied.

The manipulator suggested in this thesis is an asymmetrical parallel manipulator. Before calculation of the mobility of the manipulator one should be noticed that, if some revolute joints of a loop are parallel to each other and the rest of the revolute joints are intersecting on a point, this loop becomes an over-constrained loop and subspace number (λ) of this loop will be 5. Here we have three over-constrained loops with subspace number 5. From Alizade-Freudenstein's formula we can calculate the numbers of joint of the manipulator ($m = \sum f_i - \sum \lambda$).

$$\sum f_i = m + \sum \lambda = 5 + 3 \times 5 = 20 \quad (1)$$

The general form of a manipulator with 3 closed loops and 20 revolute joints is given in figure 9. below. The proposed manipulator and its loops can be shown below (Figure 11). One should be noticed that the proposed manipulator has both planar and spherical

links. We can separate this manipulator into two sub-systems. When two sub-systems mobility are examined separately,

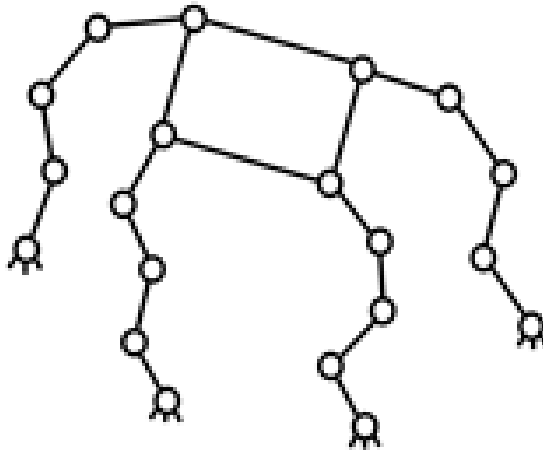


Figure 11. General form of a manipulator with 3 closed loops and 20 revolute joints

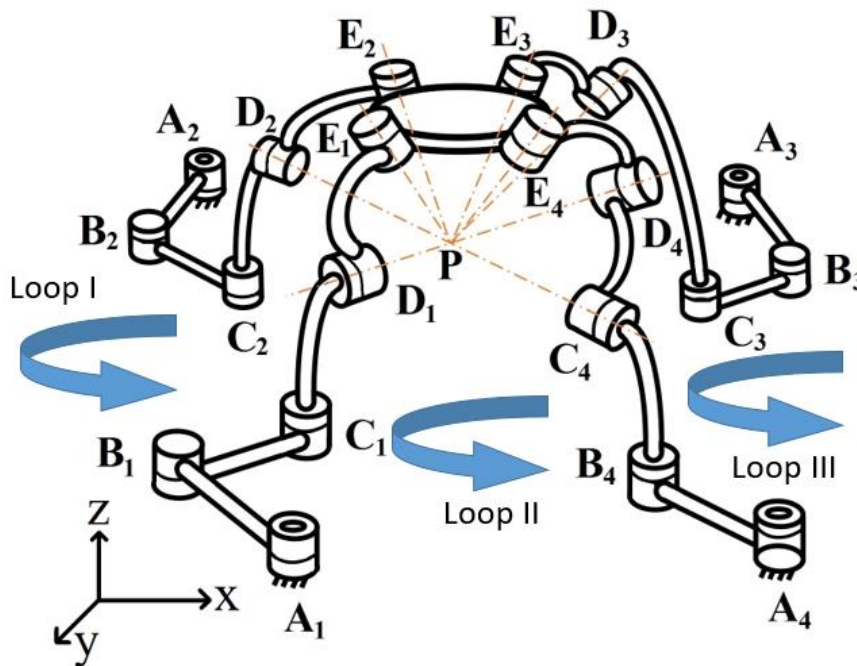


Figure 12. Loops of the manipulator

the upper part has mobility;

- 0 DoF ($m = 9 - 3 \times 3 = 0$) without imaginary joints
- 3 DoFs ($m = 12 - 3 \times 3 = 3$) with imaginary joints.

Similarly, the lower- part has mobility;

- 5 DoFs ($m = 14 - 3 \times 3 = 5$).

It seems that when the actuators are attached to the lower-part, the whole system can be controlled. Point $O_0(x, y, z)$ is selected the origin of the reference coordinate system. Four actuators are placed at first joints of all limbs (joints A_1, A_2, A_3 and A_4) and the fifth actuator is placed at the second joint of the fort limb (joint B_4).

2.2. Workspace Specification of the Manipulator

Workspace boundaries for human wrist are chosen from a study which worked on healthy people to obtain upper-limb range of motion [25]. These boundaries are given in the table 3. below. For planar motion a 240 mm x 240 mm square is selected as a workspace. The geometric center of this square is located as the ground point.

Table 3. Workspace boundaries for human wrist

Motion	Axis	Boundary	To Provide
δ_1	x	(-5 °, 45 °)	Pronation and Supination
δ_2	y	(-25 °, 35 °)	Radial and Ulnar Deviation
δ_3	z	(-35 °, 35 °)	Extension and Flexion

3. KINEMATIC ANALYSIS OF THE MANIPULATOR

To obtain motion in a given workspace without any singularity condition for active joint rates, dimensional parameters of the manipulator should be optimized. By doing inverse kinematic analysis of the manipulator constraints are obtained to use them later in optimization algorithm. Inverse kinematic analysis of the manipulator is done separately for both sub-systems.

In the spherical part, with given orientation of the end-effector for human wrist movements, we will find imaginary active joint rates for first three legs. In the leg 4, we have two spherical links with three revolute joints. This kind a combination acts like a spherical joint and a spherical joint does not have effect on the rotation of the end-effector. So, we can define leg 4 as redundant. Orientation of the end-effector, dimensional parameters and active joint rates of the upper part can be shown in figure 13.a below. After all, we can easily define upper part as a 3 DOFs spherical parallel manipulator (Figure 13.b).

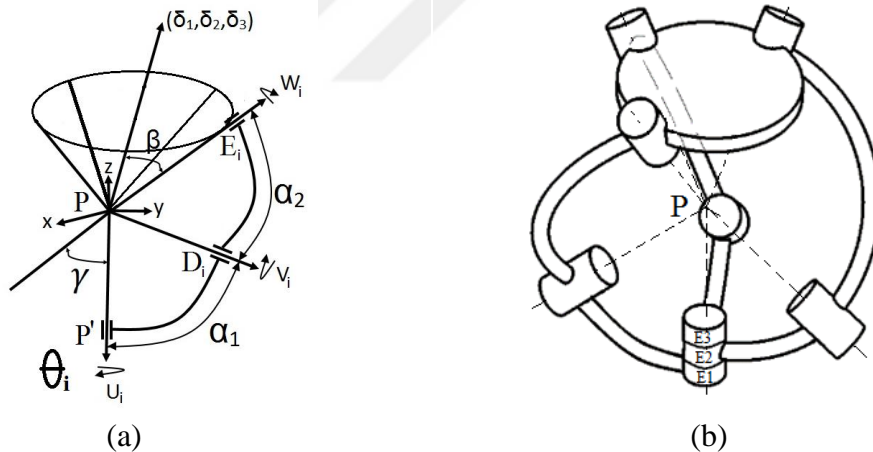


Figure 13. (a) Orientation of the end-effector, (b) Spherical part of the manipulator

For lower part, ranges obtained for imaginary active joints of spherical part are used as boundaries for first three legs. By using this new boundaries, active joint rates for lower part will be found. We know that leg 4 is independent from the orientation. Because of that position of the x-y plane trajectory of the point P can be easily controlled by attached 2 actuators on this leg. Leg 4 is acting as a 2 DOFs serial manipulator with this configuration. Dimensional parameters and active joint rates of the legs in lower part can be seen in figure 14.

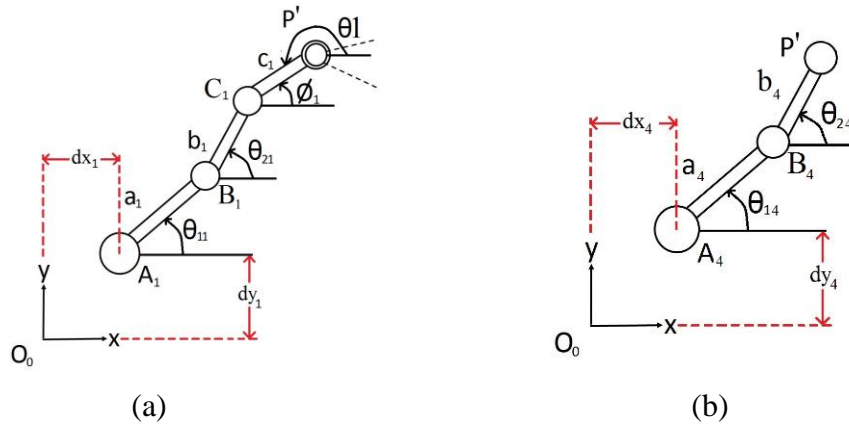


Figure 14. (a) First leg of the planar part, (b) fourth leg of the planar part

3.1. Inverse Kinematic Solutions for Upper Part

Objective function which will be used in optimization was derived by help of inverse kinematics and Jacobian equations. The orientation of the end-effector is given and rotation matrices for platform joints can be defined with following equations. Let's define unit vector \mathbf{u} as $[0,0,1]^T$.

$$\delta = \delta_z \cdot \delta_y \cdot \delta_x \quad (2)$$

Orientation of ω_i with respect to the platform is,

$$w_i^* = R_{\gamma}^z \cdot R_{\beta_i}^x \cdot [0,0,1]^T \quad (3)$$

β is the orientation of each joints around x axis with respect to z axis and is equal for all three joints and will be found with firefly algorithm. γ_i is the orientation of each joint around z axis selected for this study as 0° , 90° , 180° respectively.

$$w_i = R_{\delta_1}^x \cdot R_{\delta_2}^y \cdot R_{\delta_3}^z \cdot w_i^* \quad (4)$$

and orientation of w_i from manipulators legs can be written as,

$$w_i = R_{\theta_{1,i}}^z \cdot R_{\alpha_{1,i}}^x \cdot R_{\theta_{2,i}}^z \cdot R_{\alpha_{2,i}}^x \cdot [0,0,1]^T \quad (5)$$

Let's write Eq. 5 in matrix form,

$$\begin{pmatrix} w_x \\ w_y \\ w_z \end{pmatrix} = \begin{pmatrix} \cos(\alpha_{2,i})\sin(\alpha_{1,i})\sin(\theta_{s_{1,i}}) + \sin(\alpha_{2,i})\left(\cos(\alpha_{1,i})\cos(\theta_{s_{2,i}})\sin(\theta_{s_{1,i}}) + \cos(\theta_{s_{1,i}})\sin(\theta_{s_{2,i}})\right) \\ -\cos(\theta_{s_{1,i}})\left(\cos(\alpha_{2,i})\sin(\alpha_{1,i}) + \cos(\alpha_{1,i})\cos(\theta_{s_{2,i}})\sin(\alpha_{2,i})\right) + \sin(\alpha_{2,i})\sin(\theta_{s_{1,i}})\sin(\theta_{s_{2,i}}) \\ \cos(\alpha_{1,i})\cos(\alpha_{2,i}) - \cos(\theta_{s_{2,i}})\sin(\alpha_{1,i})\sin(\alpha_{2,i}) \end{pmatrix} \quad (6)$$

Let's eliminate $\sin(\theta_{2,i})$ from x and y components of Eq. 6, we will have,

$$w_y \cos(\theta_{s_{1,i}}) + \cos(\alpha_{2,i})\sin(\alpha_{1,i}) + \cos(\alpha_{2,i})\cos(\theta_{2,i})\sin(\alpha_{2,i}) - w_x \sin(\theta_{s_{1,i}}) = 0 \quad (7)$$

Then find $\cos(\theta_{s_{2,i}})$ from the z component of Eq. 6.

$$w_x \sin(\theta_{s_{1,i}}) = w_y \cos(\theta_{s_{1,i}}) + \cos(\alpha_{2,i}) \sin(\alpha_{1,i}) + \cos(\alpha_{1,i}) \cos(\theta_{2,i}) \sin(\alpha_{2,i}) \quad (7)$$

$$\cos(\theta_{s_{2,i}}) = - \left(w_z - \cos(\alpha_{1,i}) \cos(\alpha_{2,i}) \right) \csc(\alpha_{1,i}) \csc(\alpha_{2,i}) \quad (8)$$

Substituting Eq. (8) into Eq. (7) will give the below equation.

$$w_y \cos(\theta_{s_{1,i}}) + \left(-w_z + \cos(\alpha_{1,i}) \cos(\alpha_{2,i}) \right) \cot(\alpha_{1,i}) + \cos(\alpha_{2,i}) \sin(\alpha_{1,i}) - w_x \sin(\theta_{s_{1,i}}) = 0 \quad (9)$$

Now, let's substitute half angle formulas as, $\cos(\theta_{s_{1,i}}) = \frac{1-t_u^2}{1+t_u^2}$, $\sin(\theta_{s_{1,i}}) = \frac{2t_u}{1+t_u^2}$, $t_u = \tan(\theta_{s_{1,i}}/2)$, we get,

$$\left(-w_y - w_z \cot(\alpha_{1,i}) + \cos(\alpha_{2,i}) \csc(\alpha_{1,i}) \right) t^2 - 2w_x t + w_y - w_z \cot(\alpha_{1,i}) + \cos(\alpha_{2,i}) \csc(\alpha_{1,i}) = 0 \quad (10)$$

Solving Eq. 10 for t gives,

$$t_u = \frac{-r_1 \pm \sqrt{r_1^2 - 4 p_1 s_1}}{2 p_1} \quad (11)$$

Where,

$$p_1 = -w_y - w_z \cot(\alpha_{1,i}) + \cos(\alpha_{2,i}) \csc(\alpha_{1,i})$$

$$r_1 = -2w_x$$

$$s_1 = w_y - w_z \cot(\alpha_{1,i}) + \cos(\alpha_{2,i}) \csc(\alpha_{1,i})$$

Finally, active joint rates can be found as,

$$\theta_{s_{1,i}} = 2 \operatorname{ArcTan}(t_u) \quad (12)$$

Let's find $\sin(\theta_{s_{2,i}})$ from w_x components of Eq. 6 and find $\cos(\theta_{s_{2,i}})$ from w_z component of Eq. 6. We will have below equations.

$$\sin(\theta_{s_{2,i}}) = \csc(\alpha_{2,i}) \left(w_x \cos(\theta_{1,i}) + w_y \sin(\theta_{1,i}) \right) \quad (13)$$

$$\cos(\theta_{s_{2,i}}) = - \left(w_z - \cos(\alpha_{1,i}) \cos(\alpha_{2,i}) \right) \csc(\alpha_{1,i}) \csc(\alpha_{2,i}) \quad (14)$$

And finally, $\theta_{s_{2,i}}$ will be,

$$\theta_{s_{2,i}} = \operatorname{ArcTan}[\cos(\theta_{s_{2,i}}), \sin(\theta_{s_{2,i}})] \quad (15)$$

3.2. Inverse Kinematic Solutions for Lower Part

As mentioned before, actuators are attached to the lower part. We have 3 actuators for first 3 legs and 2 actuators for leg 4. First three legs control the orientation of the end-effector and the last leg controls its position. Let's define the x and y components of the point P as $P = (P_x, P_y)$ and orientation of the last joints (C_i) of the first three legs as ϕ_i . We found ranges for ϕ_i from upper part by setting it equal to $\theta_{s_{1,i}}$. We can define the x and y position of the third joints of first three legs from the given boundaries above.

$$C_{x,i} = c_i \cos(\phi_i) + P_x \quad (16)$$

$$C_{y,i} = c_i \sin(\phi_i) + P_y \quad (17)$$

From the position of the third joints at first three legs we can get active joint rates for first three legs ($\theta_{p_{11}}, \theta_{p_{12}}, \theta_{p_{13}}$). The vector loop equation for first three legs is given below.

$$\mathbf{O}_0 \mathbf{C}_i = \mathbf{O}_0 \mathbf{A}_i + \mathbf{A}_i \mathbf{B}_i + \mathbf{B}_i \mathbf{C}_i \quad (18)$$

Then define above equation in the fixed coordinate frame.

$$a_i \cos(\theta_{p_{1i}}) + b_i \cos(\theta_{p_{2i}}) = C_{x,i} - d_{x,i} \quad (19)$$

$$a_i \sin(\theta_{p_{1i}}) + b_i \sin(\theta_{p_{2i}}) = C_{y,i} - d_{y,i} \quad (20)$$

Let's set $C_{x,i}^* = C_{x,i} - d_{x,i}$ and $C_{y,i}^* = C_{y,i} - d_{y,i}$ and eliminate passive joint variable $\theta_{p_{2i}}$ from Eq. (19) and (20).

$$C_{x,i}^{*2} + C_{y,i}^{*2} - 2 C_{x,i}^* a_i \cos(\theta_{p_{1i}}) - 2 C_{y,i}^* b_i \sin(\theta_{p_{1i}}) + a_i^2 + b_i^2 = 0 \quad (21)$$

Rearrange Eq. (21) as,

$$p_2 \sin(\theta_{p_{1i}}) + r_2 \cos(\theta_{p_{1i}}) + s_2 = 0 \quad (22)$$

Where,

$$p_2 = -2 a_i C_{y,i}^*$$

$$r_2 = -2 a_i C_{x,i}^*$$

$$s_2 = C_{x,i}^{*2} + C_{y,i}^{*2} + a_i^2 + b_i^2$$

Then, let's substitute half angle trigonometric identities for $\cos(\theta_{p_{1i}}) = \frac{1-t_l^2}{1+t_l^2}$, $\sin(\theta_{p_{1i}}) = \frac{2t_l}{1+t_l^2}$ where $t_l = \tan(\theta_{p_{1i}}/2)$.

$$r_2 + s_2 + 2 p_2 t_l + (-r_2 + s_2) t_l^2 = 0 \quad (23)$$

Solving Eq. (23) for t gives,

$$t_l = \frac{-p_2 \pm \sqrt{p_2^2 + r_2^2 - s_2^2}}{s_2 - r_2} \quad (24)$$

Finally, active joint rates for first three legs can be found.

$$\theta_{p_{1,i}} = 2 \text{ArcTan}(t_l), i = 1, 2, 3 \quad (25)$$

For passive joint rates, we can define,

$$\text{Cos}(\theta_{p_{2i}}) = \frac{c_{x,i} - d_{x,i} - a_i \text{Cos}(\theta_{p_{1i}})}{b_i} \quad (26)$$

$$\text{Sin}(\theta_{p_{2i}}) = \frac{c_{y,i} - d_{y,i} - a_i \text{Sin}(\theta_{p_{1i}})}{b_i} \quad (27)$$

From Eq. (26) and (27),

$$\theta_{p_{2,i}} = \text{ArcTan}(\text{Cos}(\theta_{p_{2i}}), \text{Sin}(\theta_{p_{2i}})), i = 1, 2, 3 \quad (28)$$

As mentioned previous chapter, leg 4 is acting like a 2 DOFs serial manipulator. We can define end point equations of leg 4 as below.

$$P_x = a_4 \text{Cos}(\theta_{p_{14}}) + b_4 \text{Cos}(\theta_{p_{24}} - \theta_{p_{14}}) + d_{x,4} \quad (29)$$

$$P_y = a_4 \text{Sin}(\theta_{p_{14}}) + b_4 \text{Sin}(\theta_{p_{24}} - \theta_{p_{14}}) + d_{y,4} \quad (30)$$

First, elimination of the $\theta_{p_{24}}$ from above equations gives,

$$a_4^2 - b_4^2 + d_{x4}^2 + d_{y4}^2 + P_x^2 + P_y^2 - 2(d_{x4}P_x + d_{y4}P_y) + 2a_4((d_{x4} - P_x)\text{Cos}(\theta_{14}) + (d_{y4} - P_y)\text{Sin}(\theta_{14})) = 0 \quad (31)$$

Then, let's substitute half angle trigonometric identities for $\text{Cos}(\theta_{p_4}) = \frac{1-t_k^2}{1+t_k^2}$, $\text{Sin}(\theta_{p_{14}}) = \frac{2t_k}{1+t_k^2}$ where $t_k = \text{Tan}(\theta_{p_{14}}/2)$.

We get,

$$(a_4^2 - b_4^2 - 2a_4d_{x4} + d_{x4}^2 + d_{y4}^2 + 2a_4P_x - 2d_{x4}P_x + P_x^2 - 2d_{y4}P_y + P_y^2)t^2 + (4a_4d_{y4} - 4a_4P_y)t + a_4^2 - b_4^2 - 2a_4d_{x4} + d_{x4}^2 + d_{y4}^2 + 2a_4P_x - 2d_{x4}P_x + P_x^2 - 2d_{y4}P_y + P_y^2 = 0 \quad (32)$$

Solving Eq. 32 for t gives,

$$t_k = \frac{-r_3 \pm \sqrt{r_3^2 - 4p_3s_3}}{2p_3} \quad (33)$$

Here,

$$p_3 = a_4^2 - b_4^2 - 2a_4d_{x4} + d_{x4}^2 + d_{y4}^2 + 2a_4P_x - 2d_{x4}P_x + P_x^2 - 2d_{y4}P_y + P_y^2$$

$$r_3 = 4 a_4 d_{y4} - 4 a_4 P_y$$

$$s_3 = a_4^2 - b_4^2 - 2a_4 d_{x4} + d_{x4}^2 + d_{y4}^2 + 2 a_4 P_x - 2 d_{x4} P_x + P_x^2 - 2 d_{y4} P_y + P_y^2$$

Finally, first active joint rate for leg 4 can be found as,

$$\theta_{p_{14}} = 2 \text{ArcTan}(t_k) \quad (34)$$

For $\theta_{p_{24}}$, solving $\text{Cos}(\theta_{p_{24}})$ and $\text{Sin}(\theta_{p_{24}})$ from Eq. (29) and (30) respectively gives,

$$\text{Cos}(\theta_{p_{24}}) = \frac{(-d_{x4}+P_x)\text{Cos}(\theta_{p_{14}})-a_4 \text{Cos}(2\theta_{p_{14}})+(d_{y4}-P_y)\text{Sin}(\theta_{p_{14}})}{b_4} \quad (35)$$

$$\text{Sin}(\theta_{p_{24}}) = \frac{(-d_{x4}+P_x-2 a_4 \text{Cos}(\theta_{p_{14}}))+(-d_{y4}+P_y) \text{Cot}(\theta_{p_{14}})) \text{Sin}(\theta_{p_{14}})}{b_4} \quad (36)$$

From Eq. (35) and (36), $\theta_{p_{24}}$ becomes,

$$\theta_{p_{24}} = \text{ArcTan}(\text{Cos}(\theta_{p_{24}}), \text{Sin}(\theta_{p_{24}})) \quad (37)$$

4. JACOBIAN ANALYSIS OF THE MANIPULATOR

In this chapter, Jacobian analysis is done to avoid singularity conditions. Under a singularity condition, manipulators gain or loss one or more DOF which cause loss of stiffness completely [1]. In parallel manipulators, an end-effector connected to the ground with several loops. This kind of a configuration requires both active and passive joints. It is suggested that in a parallel mechanism, number of actuators equal to DOF. Actuated joint variables is denoted by \mathbf{q} vector and end-effector position is denoted by \mathbf{x} vector. Then, kinematic constraint equation can be written as,

$$\mathbf{f}(\mathbf{x}, \mathbf{q}) = 0 \quad (38)$$

Here, \mathbf{f} is an n-dimensional implicit function of \mathbf{q} and \mathbf{x} . When differentiate Eq. (38) with respect to time, we get,

$$J_x \dot{\mathbf{x}} = J_q \dot{\mathbf{q}} \quad (39)$$

In Eq. (36), J_x and J_q represent direct and inverse Jacobian matrices respectively. When following conditions happen, we can say that direct and inverse kinematic singularity occur respectively.

$$\det(J_x) = 0 \quad (40)$$

$$\det(J_q) = 0 \quad (41)$$

While Eq. (40) yields, end-effector gains 1 or more DOF which means the manipulator has no resistance to forces or moments in some directions. While Eq. (41) yields, end-effector loses 1 or more DOF which means manipulator has infinite resistance to forces or moments in some directions. While both Eq. (40) and (41) yield a combined singularity occurs. With this type of singularity, end-effector can be locked or go infinitesimal motion.

Jacobian matrices can be characterized by using a parameter called condition number. Condition number of an any A matrix can be defined as below.

$$c = \|A\| \|A^{-1}\| \quad (42)$$

$\| \cdot \|$ sign denotes the norm of a matrix. Condition number is a link lengths and manipulator configuration depending measurement. Condition number indicates farness of the manipulator from singularity. The value of the condition number is wanted to be 1. Jacobian analysis of the proposed manipulator is examined separately for both sub-systems.

4.1. Jacobian Analysis of the Upper Part

Let's angular velocity of end effector be as $\boldsymbol{\omega} = [\omega_x \ \omega_y \ \omega_z]^T$ and input angle velocities of the spherical part be as $\dot{\boldsymbol{\theta}} = [\dot{\theta}_{1,i} \ \dot{\theta}_{2,i} \ \dot{\theta}_{3,i}]^T$. Jacobian relation between them,

$$\mathbf{J}_{s_x} \boldsymbol{\omega} = \mathbf{J}_{s_q} \dot{\boldsymbol{\theta}} \quad (43)$$

Resulting end-effector velocity equation becomes,

$$\boldsymbol{\omega} = u_i \cdot \dot{\theta}_{1,i} + v_i \cdot \dot{\theta}_{2,i} + w_i \cdot \dot{\theta}_{3,i} \quad (44)$$

Let's dot product both sides in Eq. (44) with $v \times w$. By using following relations $a \cdot (b \times c) = b \cdot (c \times a) = c \cdot (a \times b)$, we will have,

$$\boldsymbol{\omega} \cdot (v_i \times w_i) = u_i \cdot (v_i \times w_i) \cdot \dot{\theta}_{1,i} \quad (45)$$

Let's define $R_B^A = R_{\delta_3^z} \cdot R_{\delta_2^y} \cdot R_{\delta_1^z}$ as and for a rigid body skew-symmetric matrix angular velocity matrix can be calculated as below.

$$\boldsymbol{\Omega} \equiv \dot{R}_B^A R_B^{A^{-1}} = \begin{pmatrix} 0 & -\omega_z & \omega_y \\ \omega_z & 0 & -\omega_x \\ -\omega_y & \omega_x & 0 \end{pmatrix} \quad (46)$$

And angular velocity components become,

$$\omega_{x,i} = \text{Cos}(\delta_2) \text{Cos}(\delta_3) \dot{\delta}_1 - \text{Sin}(\delta_3) \dot{\delta}_2 \quad (47)$$

$$\omega_{y,i} = \text{Cos}(\delta_2) \text{Sin}(\delta_3) \dot{\delta}_1 + \text{Cos}(\delta_3) \dot{\delta}_2 \quad (48)$$

$$\omega_{z,i} = -\text{Sin}(\delta_2) \dot{\delta}_1 + \dot{\delta}_3 \quad (49)$$

Also we know that from geometry of spherical part,

$$\mathbf{u} = [0,0,1]^T \quad (50)$$

$$\mathbf{v} = R_{\theta_{1,i}^z} \cdot R_{\alpha_{1,i}^x} \cdot [0,0,1]^T \quad (51)$$

$$\mathbf{w}_i = R_{\theta_{1,i}^z} \cdot R_{\alpha_{1,i}^x} \cdot R_{\theta_{2,i}^z} \cdot R_{\alpha_{2,i}^x} \cdot [0,0,1]^T \quad (52)$$

When we substitute this equations into Eq. 45 we get \mathbf{J}_{s_x} and \mathbf{J}_{s_q} .

$$\mathbf{J}_{s_q} = \begin{pmatrix} J_{s_{q1,1}} & 0 & 0 \\ 0 & J_{s_{q2,2}} & 0 \\ 0 & 0 & J_{s_{q3,3}} \end{pmatrix} \quad (53)$$

Where,

$$J_{s_{q1,1}} = \text{Sin}(\alpha_{1,1}) \text{Sin}(\alpha_{2,1}) \text{Sin}(\theta_{2,1}),$$

$$J_{s_{q2,2}} = \text{Sin}(\alpha_{1,2}) \text{Sin}(\alpha_{2,2}) \text{Sin}(\theta_{2,2}) \text{ and}$$

$$J_{s_{q3,3}} = \text{Sin}(\alpha_{1,3})\text{Sin}(\alpha_{2,3})\text{Sin}(\theta_{2,3}).$$

$$J_{s_x} = \begin{pmatrix} J_{s_{x1,1}} & J_{s_{x2,1}} & J_{s_{x3,1}} \\ J_{s_{x1,2}} & J_{s_{x2,2}} & J_{s_{x3,2}} \\ J_{s_{x1,3}} & J_{s_{x2,3}} & J_{s_{x3,3}} \end{pmatrix} \quad (54)$$

Where,

$$J_{s_{x1,i}} = \text{Sin}(\alpha_{2,i})(\text{Sin}(\alpha_{1,i})\text{Sin}(\delta_2)\text{Sin}(\theta_{2,i}) - \text{Cos}(\delta_2)(\text{Cos}(\delta_3 - \theta_{1,i})\text{Cos}(\theta_{2,i}) + \text{Cos}(\alpha_{1,i})\text{Sin}(\delta_3 - \theta_{1,i})\text{Sin}(\theta_{2,i}))),$$

$$J_{s_{x2,i}} = \text{Sin}(\alpha_{2,i})(\text{Cos}(\theta_{2,i})\text{Sin}(\delta_3 - \theta_{1,i}) - \text{Cos}(\alpha_{1,i})\text{Cos}(\delta_3 - \theta_{1,i})\text{Sin}(\theta_{2,i})) \text{ and}$$

$$J_{s_{x3,i}} = -\text{Sin}(\alpha_{1,i})\text{Sin}(\alpha_{2,i})\text{Sin}(\theta_{2,i}).$$

4.2. Jacobian Analysis of the Lower Part

Let the output vector be as $\mathbf{x}=[P_x \ P_y \ \phi_1 \ \phi_2 \ \phi_3]$ and input vector of the lower part be as $\mathbf{q}=[\theta_{11}, \theta_{12}, \theta_{13}, \theta_{14}, \theta_{24}]$ and where loop-closure equation of leg 1,2,3 can be written as follow,

$$\mathbf{A}_i \mathbf{P}' + \mathbf{P}' \mathbf{C}_i = \mathbf{A}_i \mathbf{B}_i + \mathbf{B}_i \mathbf{C}_i \quad (55)$$

When derivatives of the both sides with respect to time is taken in loop-closure equation, consider V_P is the velocity of point P' . To be eliminate the passive joint variable ($\dot{\theta}_{2i}$), both side of loop-closure equation is dot-multiplied by b_i leads to,

$$b_{i,x}V_{p,x} + b_{i,y}V_{p,y} + (c_{i,x}b_{i,y} - c_{i,y}b_{i,x}) \dot{\phi}_i = (a_{i,x}b_{i,y} - a_{i,y}b_{i,x}) \dot{\theta}_{1i} \quad (56)$$

The loop-closure equation for leg 4 can be written as

$$\mathbf{A}_4 \mathbf{P}' + \mathbf{P}' \mathbf{B}_4 = \mathbf{A}_4 \mathbf{B}_4 \quad (57)$$

Similarly, taking derivative of loop-closure equation for leg 4 with respect to time and separating vector parts leads followings,

$$V_{p,x} = -a_{4,y} \dot{\theta}_{14} - b_{4,y}(\dot{\theta}_{24} - \dot{\theta}_{14}) \quad (58)$$

$$V_{p,y} = a_{4,x} \dot{\theta}_{14} + b_{4,x}(\dot{\theta}_{24} - \dot{\theta}_{14}) \quad (59)$$

From Eq. (56), (58) and (59) Jacobian matrices can be written as,

$$J_p = J_p q^{-1} J_p x \quad (60)$$

Where,

$$Jp_x = \begin{pmatrix} Jp_{x,11} & Jp_{x,12} & Jp_{x,13} & 0 & 0 \\ Jp_{x,21} & Jp_{x,22} & 0 & Jp_{x,24} & 0 \\ Jp_{x,31} & Jp_{x,32} & 0 & 0 & Jp_{x,35} \\ 1 & 0 & 0 & 0 & 0 \\ 0 & 1 & 0 & 0 & 0 \end{pmatrix} \quad (61)$$

$$Jp_q = \begin{pmatrix} Jp_{q,11} & 0 & 0 & 0 & 0 \\ 0 & Jp_{q,22} & 0 & 0 & 0 \\ 0 & 0 & Jp_{q,33} & 0 & 0 \\ 0 & 0 & 0 & Jp_{q,44} & Jp_{q,45} \\ 0 & 0 & 0 & Jp_{q,54} & Jp_{q,55} \end{pmatrix} \quad (62)$$

Here, components of the Jacobian matrices can be written as,

$J_{P,x,11}=b_{1,x}$	$J_{P,q,11}= a_{1,x} b_{1,y} - a_{1,y} b_{1,x}$
$J_{P,x,12}=b_{1,y}$	$J_{P,q,22}= a_{2,x} b_{2,y} - a_{2,y} b_{2,x}$
$J_{P,x,13}=b_{1,y} c_{1,x} - b_{1,x} c_{1,y}$	$J_{P,q,33}= a_{3,x} b_{3,y} - a_{3,y} b_{3,x}$
$J_{P,x,21}=b_{2,x}$	$J_{P,q,44}= -a_{4,y} + b_{4,y}$
$J_{P,x,22}=b_{2,y}$	$J_{P,q,45}= -b_{4,y}$
$J_{P,x,24}=b_{2,y} c_{2,x} - b_{2,x} c_{2,y}$	$J_{P,q,54}= a_{4,x} - b_{4,x}$
$J_{P,x,31}=b_{3,x}$	$J_{P,q,55}=b_{4,x}$
$J_{P,x,32}=b_{3,y}$	
$J_{P,x,35}=b_{3,y} c_{3,x} - b_{3,x} c_{3,y}$	

5. DIMENSIONAL OPTIMIZATION OF THE MANIPULATOR

We can examine mechanisms kinematically into two ways. One of them is workspace specification with selected dimensional parameters which includes direct kinematic solutions and the other is dimensional parameter specification with desired workspace which includes inverse kinematic solutions. In this thesis, we specified the workspace boundaries for rehabilitation purpose. To fulfill these boundaries without any singularity condition we need to determine dimensional parameters. In kinematic synthesis of the manipulators 3 main ways are used. These methods are,

- Function generation
- Motion generation
- Path generation

Function generation is a method to establish a relation between input and output rates of mechanisms with a function. From this relation, mechanisms properties are found to provide the desired function. In this method the relation will be set by using functions. There are two main ways to solve function generation problems. These are approximation and optimization methods.

- Approximation Methods
 - + Interpolation Methods
 - + Least Square Method
 - + Chebyshev Method
- Optimization Methods
 - + Linear Optimization (Newton Raphson Method etc.)
 - + Non-Linear Optimization (Genetic Algorithms, Firefly Algorithms etc.)

Consider our input rate θ is a function of x as $\theta=f(x)$ and output rate ϕ is a function of y as $\phi=f(y)$. Also y is a function of x as $y=f(x)$. The aim of the function generation is to make a relationship between θ and ϕ by using function $y=f(x)$. After that, ranges for x , θ , ϕ should be determined. Graphical representation for function generation is given in figure 15 below.

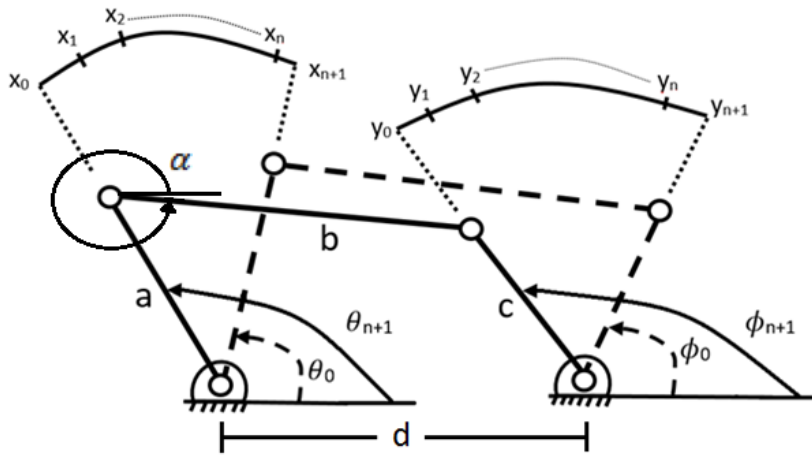


Figure 15. Graphical representation of function generation

Motion generation is another method to find mechanisms architectural parameters. In motion generation, we have the position and orientation of end effector of mechanisms for desired points (3, 4 or 5 points) and we aim to calculate architectural parameters of the mechanism. Consider we have a four bar as figure 16. below.

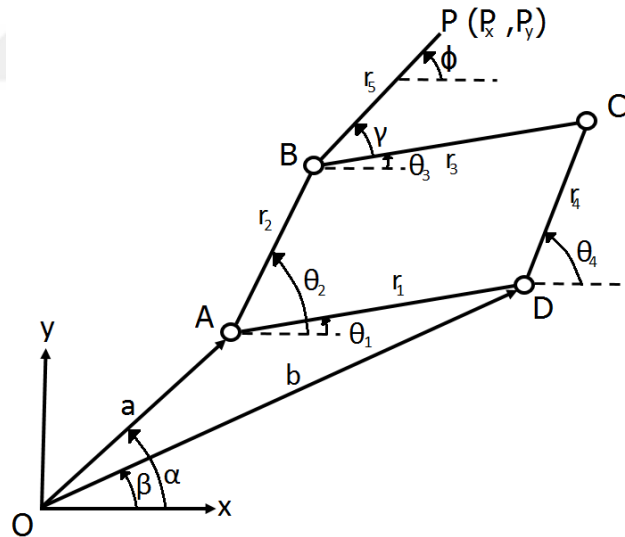


Figure 16. Fourbar for motion generation

We know only end effector's position and orientation (P_x , P_y and ϕ) for some desired points and our end effector moves on these desired points. To provide this motion we need to determine architectural parameters (a , b , r_1 , r_2 , r_3 , r_4 and r_5) and their orientations (α , β , γ , ϕ , θ_1 , θ_2 , θ_3 and θ_4) with respect to the reference coordinate system O.

The aim of the path generation is specifying the dimensional parameters and the output rate of the mechanism to provide a point on the end-effector follows the desired points. In this thesis, dimensional parameters are wanted to determine with given path in the workspace boundaries. But, one should be noticed that we have large number of path points with highly nonlinear equations. In path generation synthesis problems with more than 5 points, analytical methods remain incapable. At this point, numerical methods become a part of activity to obtain mechanism dimensions with large number of desired path points. In literature, researchers usually used evolutionary algorithms to overcome synthesis problems for mechanism. Z. Nariman et al. [26] used hybrid multi-objective genetic algorithms for Pareto optimum synthesis of four bar mechanism with minimizing two objective functions (tracking error and transmission angle error) at the same time. Lin W [27] compounded two different evolutionary algorithm named differential evolution (DE) and real-valued genetic algorithm (RGA) to synthesize four bar mechanism with several design parameters for 6, 10 and 18 points in different cases. Only considered constraints of his work were the Grashof condition, design parameters within specified ranges, rotation range of the crank and relation between input angle and crank. Acharyya S. K. and Mandal M. [28] applied three different type of evolutionary algorithm (GA, PSO and DE) to minimize the error between desired and obtained coupler curve in four bar path generation synthesis. Researcher also compared these methods between each other and selected the best one. H Yu., et al. [29] presented a computer method which uses coupler-angle function curve to synthesize a four bar mechanism. They practiced a two DoFs additional mechanism to transform coupler-points of the given path to a coupler-angle function curve. They also presented a software which give opportunity to users to define up to 20 points for path. Bulatovic R. R. and Djordjevic S. R. [30] used a direct searching method for four bar synthesis named Hooke-Jeeves's which compares its values at each iteration and changes parameters in order to described objective function. They proposed that the used algorithm in their research does not depend on the preliminary selected variables. Researchers showed a four bar example which coupler point draw a straight line.

There have been applied several ways to optimize parallel manipulators by using indexes such as specified conditioning index (SCI), global conditioning index (GCI) and global dynamic conditioning index (GDCI). There are also several algorithms and methods were applied to solve optimization problems of parallel manipulators such as multi-criteria analysis controlled random search, linear actuation method, Monte Carlo method, exhaustive search minimization algorithm, firefly algorithm, genetic algorithms etc. Huang T. et. al. [31] bounded the workspace of 2-DOF parallel manipulators in a rectangular area by using specified conditioning index. Further Olds K.C. [32] developed a new approach for global indices to solve optimization problems for parallel robots. Dou R. [33] investigated the global conditioning index (GCI), the

global velocity index (GVI), and global stiffness index (GSI) of 3-RRR parallel manipulators and represented corresponding atlases. Based on these atlases he determined geometric parameters without dimensions for 3-RRR parallel manipulators. Lou, Y. J., et. all. [34] utilized dexterity index to characterize the effectiveness of the workspace. In their study, the inverse condition number of Jacobian matrix was used in order to measure dexterity.

Optimization on medical robots is a very vital issue because of the task is human body. Stan, S. [35] summarized the mono-objective optimal design procedure using the workingspace for the parallel robot and the numerical optimality criterion. Kinematic performance optimization was performed to maximize the workspace of the mini parallel robot. Optimization was performed using Genetic Algorithms. Likewise, Stan, S. et.al. [36] used Generic Algorithms to optimize the geometric parameters of a planar medical parallel robot. Badescu, M. And Mavroidis, C. [37] calculated several indices by using Monte Carlo Methods for workspace optimization of upu and ups parallel platforms with three legs. Stock, M., and Miller, K. [38] examined the mobility, workspace and manipulability characteristics of a linear deltas robots by using the exhaustive search minimization algorithm. They use a sophisticated search algorithm to reliably locate possible design candidates in a four-dimensional parameter space. Gao, Z., and Zhang, D. [39] applied the particle swarm algorithm to maximize the workspace volume of a new parallel mechanism with 3 DoFs.

5.1. Optimization Method (Firefly Algorithm)

In this study, Firefly algorithm was used to optimize dimensional parameters of purposed manipulator. Firefly algorithm is developed by Yang [41] and is a nature inspired metaheuristic algorithm [42]. In firefly algorithm, each agents (fireflies) propagate lights and brighter ones pull other fireflies in close [41]. Few researchers in robotics used firefly algorithm to overcome optimization problem for their mechanisms. Nedic N. et. al. [42] proposed a cascade load force control design for a parallel robot platform. They used Firefly algorithm for parameter searching.

Researchers who worked with Firefly Algorithm in robotics indicate that [42, 43]:

- Firefly algorithm is very effective in nonlinear optimization tasks and performs better than other metaheuristic algorithms.
- Firefly Algorithm is independent from the complexity of problems.
- Firefly Algorithm has a better rate of convergence.
- Firefly Algorithm gives values faster than other algorithms.

- Firefly Algorithm can solve highly nonlinear, multimodal problems with high efficiency.

In the study, local minimum solutions are searched and it is taught that it is sufficient for this study. Optimization is performed by separating the workspace into small pieces to operate the manipulator into whole workspace. Genetic algorithm was also tested in this study. It has seen that Genetic algorithm stay slow comparing to Firefly algorithm. Firefly algorithm was applied our optimization problem as follow. Parameters used in the algorithm were selected by taking into consideration of Lukasik S. and Zak S.'s research about firefly algorithm [44]. Here, n_f denotes the population of fireflies and n_c is the number of coordinates and signs the number of variables which are expected to be optimized. γ is called approach speed or absorption coefficient and it states multifariousness with escalating distance from interacted firefly [44]. β_0 is the attractiveness, it indicates the capability of a firefly to draw in other fireflies. α is defined as randomness and it remarks the how much fireflies move randomly. S denotes to scale of randomness α and randomness is multiplied with scale at each iteration. Light intensity of a firefly is measured by I and it directly impresses the movement of fireflies. Here $f(x_i)$ is the objective function and x_i is the solution for parameters which are wanted to be optimized at each iteration. Finally $r_{i,j}$ is the monotonically decreasing function of the distance between fireflies.

```

Objective function  $f(x_i)$ ,
 $x_i = (\text{Define the parameters to be optimized})^T$ , where
 $f(x_i) = (\text{Define the objective function})$ 
Generate initial population of fireflies  $x_i (i = 1, 2, \dots, n_f)$ .
Light intensity  $I$  at  $x_i$  is determined by  $f(x_i)$ 
Define light absorption coefficient  $\gamma$ 
for ( $m_i; 1, \text{MaxGen}$ )
  for  $i = 1: n_f$ 
    for  $j = 1: n_f$ 
      if ( $I_i < I_j$ ),
         $r_{i,j} = \sqrt{\text{Sum} [(x_{k,i} - x_{k,j})^2, (k, 1, n_c)]}$ ;
        Do  $\left[ x_{k,i} = x_{k,i} + \frac{\beta_0 S_k}{1 + \gamma r_{i,j}^2} (x_{k,j} - x_{k,i}) + \alpha S(\text{Random}[] - 0.5), \{k, 1, n_c\} \right]$ ,
        (move firefly i towards to j)
      else Do  $\left[ x_{k,i} = x_{k,i} + \alpha S(\text{Random}[] - 0.5), \{k, 1, n_c\} \right]$ , (move firefly random)
      end if
    end for j
  end for i
  Evaluate new solutions of  $f(x_i)$  and update light intensity
  end for j
  end for i
  Rank the fireflies and find the current global best  $g^*$ 
end for

```

5.2. Optimization of Upper Part

Dimensional parameters which are wanted to be optimize for the spherical part is,

- $\alpha_{1,i}$, length of the first spherical links (selected equal for each leg)
- $\alpha_{2,i}$, length of the second spherical links (selected equal for each leg)
- β , orientation of each joints around x axis with respect to z axis (selected equal for each leg)

Selected Firefly Algorithm parameter are given on table 4. below.

Table 4. Selected Firefly Algorithm parameters for spherical part

nr	nc	γ	β_0	α	S
50	3	0.8	0.8	0.1	1

Parameters used in the algorithm were selected by taking into consideration of Lukasik S. and Zak S.'s research about firefly algorithm [44]. Constraints are selected as which make imaginary active joints and passive joints indefinite or imaginary and which make determinant of the inverse and direct Jacobian matrices are zero. Let's remember Eq. (12) ($\theta_{s_{1,i}} = 2 \text{ ArcTan}(t)$) depend on t whose equation is $t = \frac{-b \pm \sqrt{b^2 - 4ac}}{2a}$. Here the terms which are capable to make t undefined are selected as constraints. These constraints can be listed as follow,

$$C_1 = b^2 - 4ac \geq 0$$

$$C_2 = a \neq 0.$$

For passive joints, let's remember their equation ($\theta_{s_{2,i}} = \text{ArcTan}[\text{Cos}(\theta_{s_{2,i}}), \text{Sin}(\theta_{s_{2,i}})]$). For ArcTan function that is in form $z = \text{ArcTan}(x, y)$ gives the arc tangent of y/x. So, we can define our constraint for passive joints as,

$$C_3 = \text{Cos}(\theta_{s_{2,i}}) \neq 0.$$

From inverse and direct Jacobian matrices, two more constraints can be defined as,

$$C_4 = \det(Js_x) \neq 0$$

$$C_5 = \det(Js_q) \neq 0.$$

Also, some ranges are determined for dimensional parameters to keep them in reasonable values. After specification of the constraints, objective function is selected

as minimization of the dimensional parameters and maximization of the condition numbers for both direct and inverse Jacobian matrices.

$$OBJ_s = \frac{100}{\sqrt{1+\alpha_1^2+\alpha_2^2+\beta^2}} Length(Cs_q)Length(Cs_x) \quad (63)$$

Here Cs_q and Cs_x represent the condition numbers of inverse and direct Jacobian matrices respectively. After necessary iterations, dimensional parameters are found (Table 5). Here, we combined the upper and lower part of the manipulator to minimize imaginary input ranges.

Table 5. Optimized dimensional parameters for spherical part

	α_1 (Rad)	α_2 (Rad)	β (Rad)
Optimized Values	0.938802	1.34815	1.39626

5.3. Optimization of Lower Part

Dimensional parameters which are wanted to be optimize for the planar part is,

- a_i , length of the first planar links
- b_i , length of the second planar links
- c_i , length of the second planar links
- $d_{x,i}$, x axis distance to the ground point of first joints
- $d_{y,i}$, y axis distance to the ground point of first joints

Selected Firefly Algorithm parameter are given on table 6 below.

Table 6. Selected Firefly Algorithm parameters for planar part

nr	nc	γ	β_0	α	S
30	11	0.2	0.8	0.1	20

Constraints are selected as which make active and passive joints indefinite or imaginary and which make determinant of the inverse and direct Jacobian matrices are zero. As seen in Eq. (31) depend on t whose equation is $t = \frac{-e_1 \pm \sqrt{e_1^2 + e_2^2 - e_3^2}}{e_3 - e_2}$. Here the terms which are capable to make t undefined are selected as constraints. These constraints can be listed as follow,

$$C_1 = e_1^2 + e_2^2 - e_3^2 \geq 0, C_2 = e_3 - e_2 \neq 0.$$

For passive joints, let's remember their equation ($\theta_{p_{2,i}} = \text{ArcTan}(\text{Cos}(\theta_{p_{2,i}}), \text{Sin}(\theta_{p_{2,i}})), i = 1, 2, 3$). For ArcTan function that is in form $z = \text{ArcTan}(x, y)$ gives the arc tangent of y/x . So, we can define our constraint for passive joints as,

$$C_3 = \text{Cos}(\theta_{p_{2,i}}) \neq 0.$$

For leg 4, let's remember active joint equations ($\theta_{p_{14}} = 2 \text{ArcTan}(t), \theta_{p_{24}} = \text{ArcTan}(\text{Cos}(\theta_{p_{24}}), \text{Sin}(\theta_{p_{24}}))$ and $t = \frac{-b \pm \sqrt{b^2 - 4ac}}{2a}$). Active joints constraints from leg 4 are listed below.

$$C_4 = b^2 - 4ac \geq 0, C_5 = a \neq 0, C_6 = \text{Cos}(\theta_{p_{24}}) \neq 0$$

From inverse and direct Jacobian matrices, two more constraints can be defined as,

$$C_7 = \det(Jp_x) \neq 0, C_8 = \det(Jp_q) \neq 0$$

Also, some ranges are determined for dimensional parameters to keep them in reasonable values. In addition to this constraints, to keep the ground points of the legs out the workspace and away from the each other additional constraints are added. After specification of the constraints, objective function is selected as minimization of the dimensional parameters and maximization of the condition numbers for both direct and inverse Jacobian matrices.

$$OBJp = \frac{100}{\sqrt{1+a^2+b^2+c^2+\sum_i^4 d_{x,i}^2+\sum_i^4 d_{y,i}^2}} \text{Length}(Cp_q) \text{Length}(Cp_x) \quad (64)$$

Here Cp_q and Cp_x represent the condition numbers of inverse and direct Jacobian matrices respectively. After necessary iterations, dimensional parameters are found separately for each leg (Table 7). Optimized and assembled manipulator can be seen in figure 17. More detailed figures are given in Appendix B.

Table 7. Optimized dimensional parameters for planar part

(mm)	a1	b1	c1	dx1	dy1	dx2	dy2	dx3	dy3	dx4	dy4
Optimized Values	437	431	71	-271	-349	405	42	493	2	224	-224
	a2	a2	c2	a3	b3	c3	a4	b4			
	540	607	74	554	648	44	328	241			

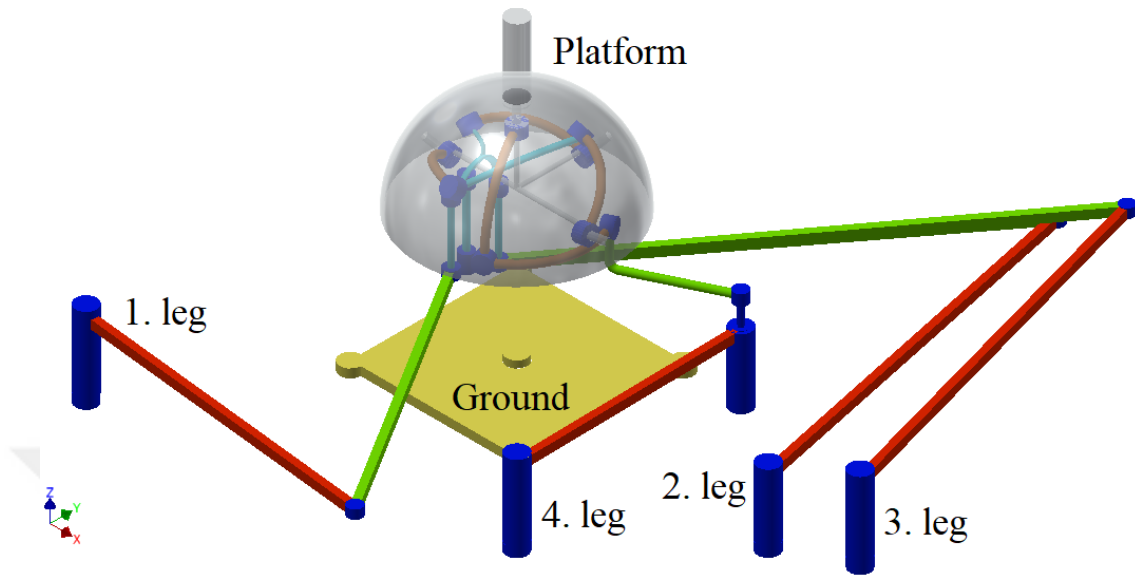


Figure 17. Optimized and assembled manipulator

6. TEST OF OPTIMIZED PARAMETERS WITH DESIRED MOVEMENTS INTO WORKSPACE

The presented manipulator in this paper was modelled and simulated by the help of MATLAB Simmechanics package. In this section, it was checked whether the obtained optimum dimensional parameters provided the workspace. With giving platform movements, it was tested that input variables are continuous. Simulations are done separately for both sub-systems. Obtaining active joint rates from upper part will be the boundaries for lower part.

6.1. Simulations of Upper Part

In the tests for spherical part it is checked whether rotations around three principal axes provided. Behaviors of three imaginary active joints are examined with specified movements by using workspace boundaries which were originated from rotation around x, y and z axes. In this chapter, only position control of the manipulator is done by using MATLAB software. Firstly, manipulator modelled in 3D by using Inventor software. Then, assembled version of the manipulator is exported for MATLAB software. Input of the inverse kinematic functions block is connected to the input values for platform orientation and output of the inverse kinematic functions block is connected to the input of the active joint blocks. This block is a MATLAB function block and includes dimensional parameters of the upper part and its inverse kinematic equations for imaginary active joints. Scopes are connected to the output of the imaginary active joints to observe the behaviors of them. Additional 3 control block added to observe the rotation angle of the platform around x, y and z axes. This control blocks are also modelled by adding three extra joint in Inventor software. Given and obtained rotation around axes are observed from these blocks.

Motion control of the manipulator is done by using PID blocks. PID control blocks were established for three imaginary active joints. A PID block was tuned by using simmechanics tools for one linked system and obtained P, I and D values ($P = 11.8$, $I = 74.8$, $D = 0.413$) were used for all three active joints. It was accepted that effect of other joints on the model was disturbance. Twelve different test results can be viewed as followed figures. Table 8 shows that the input variables of the manipulator for three different sets of simulations and figure 18 shows these simulation results. The obtained simulation results show that the dimensional parameters obtained with firefly algorithm provide the workspace completely and the manipulator operated without any singularity condition for spherical part.

Table 8. Simulations on spherical part

Set 1			
	δ_1	δ_2	δ_3
A	Sin wave (Amplitude: 0.4, Frequency:1 rad/sec)	-30 Degree	-40 Degree
B	Sin wave (Amplitude: 0.4, Frequency:1 rad/sec)	-30 Degree	40 Degree
C	Sin wave (Amplitude: 0.4, Frequency:1 rad/sec)	40 Degree	-40 Degree
D	Sin wave (Amplitude: 0.4, Frequency:1 rad/sec)	40 Degree	40 Degree

Set 2			
	δ_1	δ_2	δ_3
A	-10 Degree	Sin wave (Amplitude: 0.4, Frequency:1 rad/sec)	-40 Degree
B	-10 Degree	Sin wave (Amplitude: 0.4, Frequency:1 rad/sec)	40 Degree
C	50 Degree	Sin wave (Amplitude: 0.4, Frequency:1 rad/sec)	-40 Degree
D	50 Degree	Sin wave (Amplitude: 0.4, Frequency:1 rad/sec)	40 Degree

Set 3			
	δ_1	δ_2	δ_3
A	-10 Degree	-30 Degree	Sin wave (Amplitude: 0.4, Frequency:1 rad/sec)
B	-10 Degree	40 Degree	Sin wave (Amplitude: 0.4, Frequency:1 rad/sec)
C	50 Degree	-30 Degree	Sin wave (Amplitude: 0.4, Frequency:1 rad/sec)
D	50 Degree	40 Degree	Sin wave (Amplitude: 0.4, Frequency:1 rad/sec)

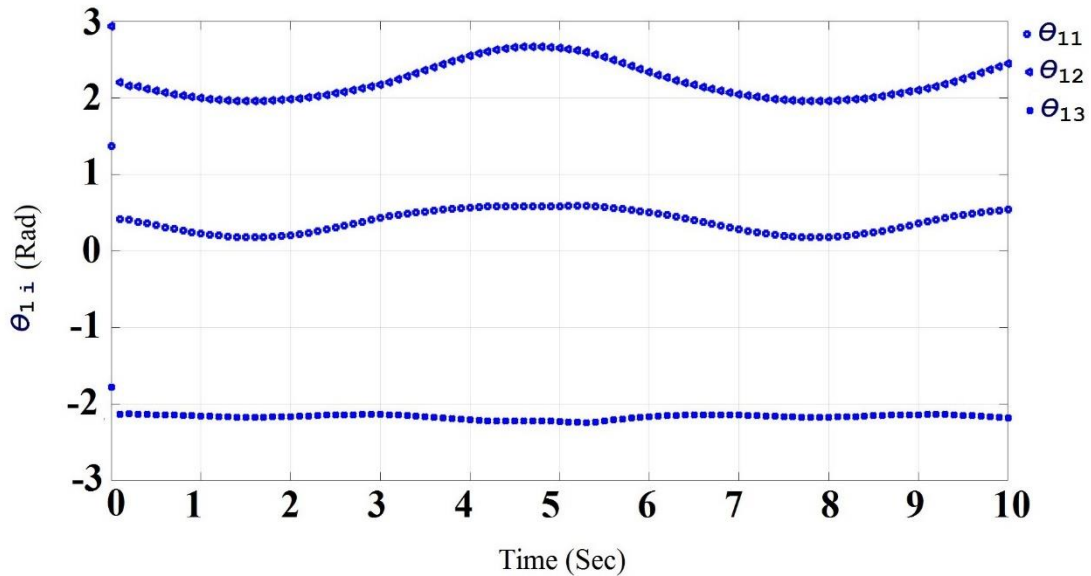


Figure 18 (a). Set 1, simulation A

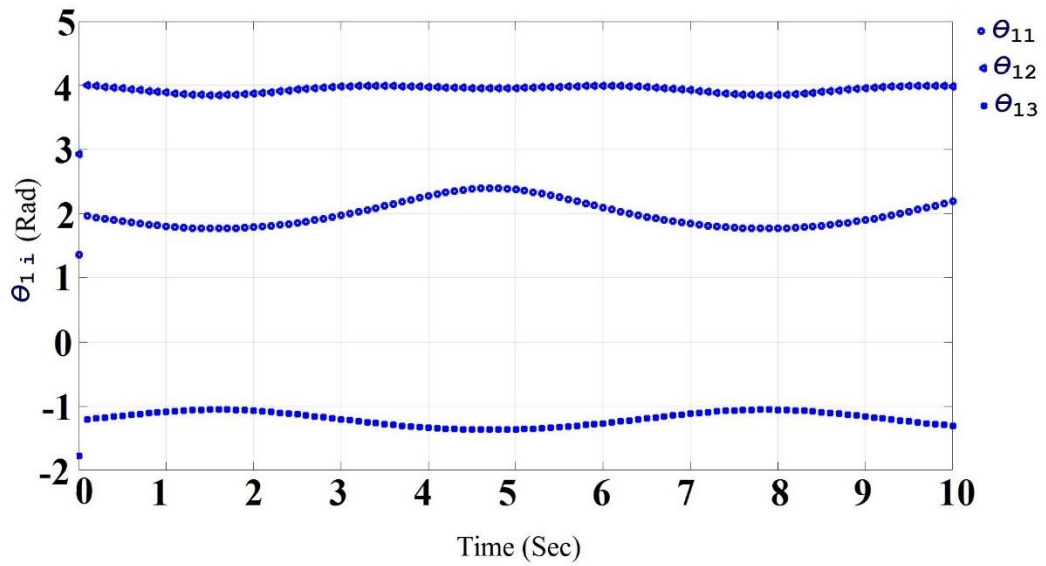


Figure 18 (b). Set 1, simulation B

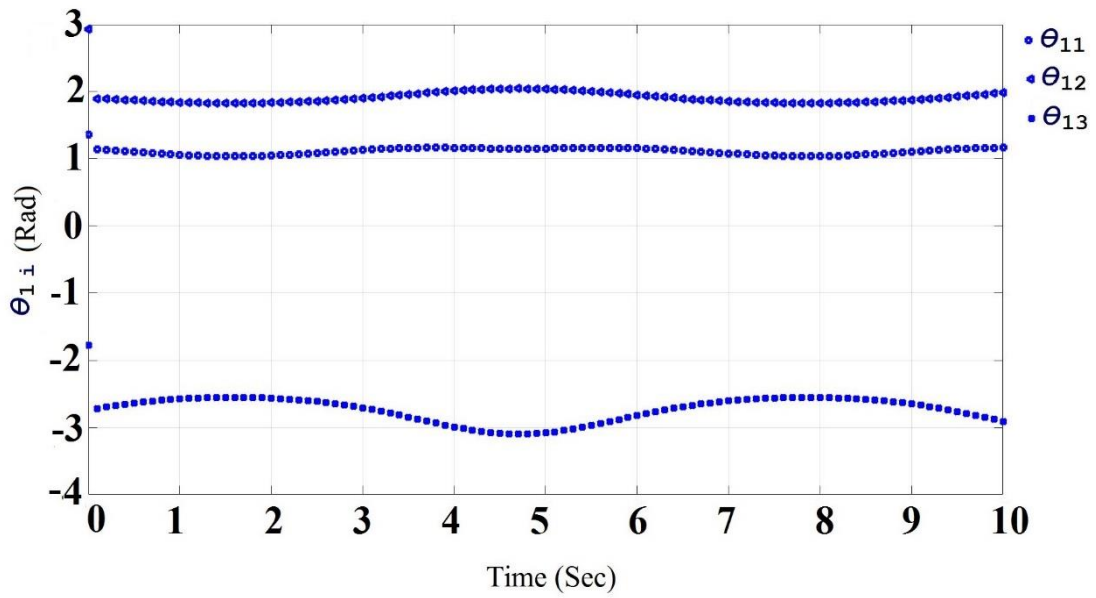


Figure 18 (c). Set 1, simulation C

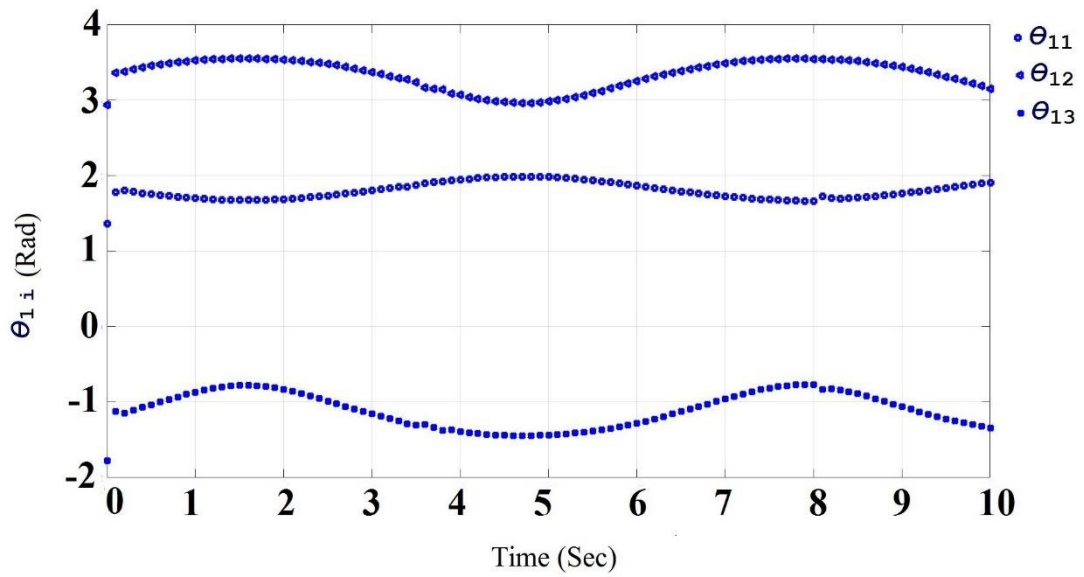


Figure 18 (d). Set 1, simulation D

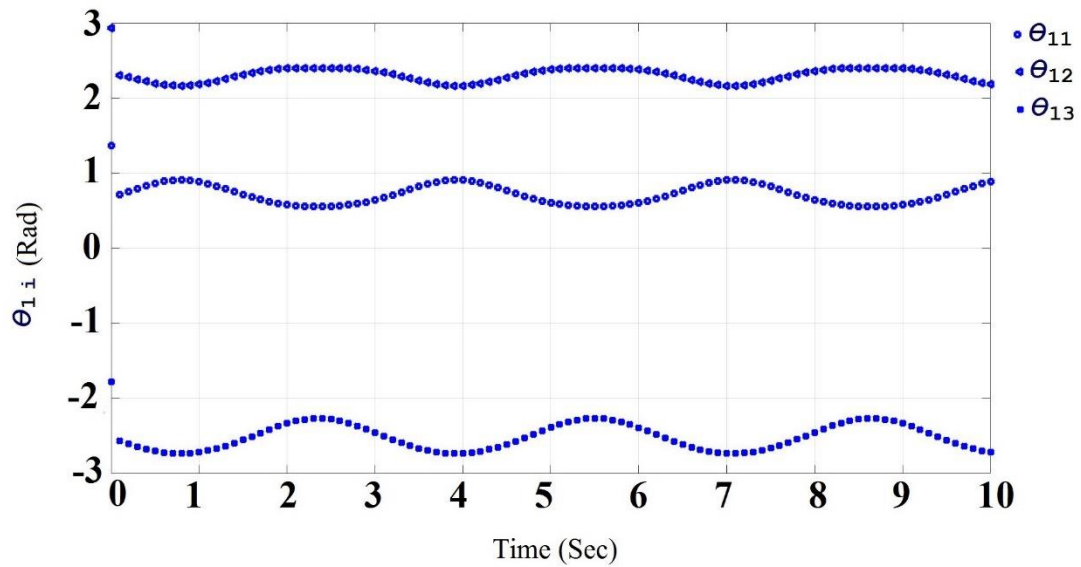


Figure 18 (e). Set 2, simulation A

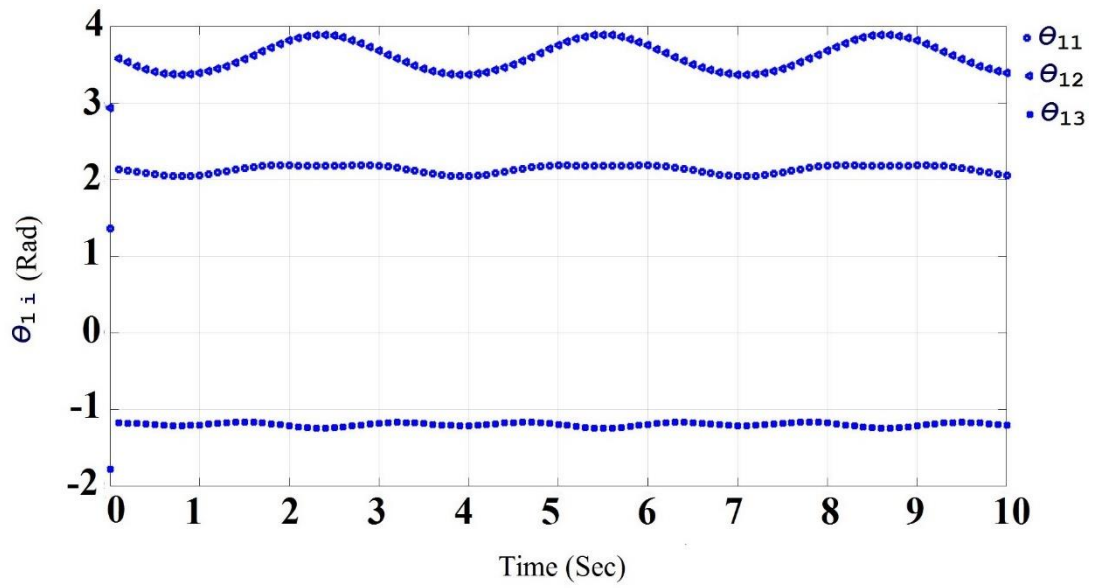


Figure 18 (f). Set 2, simulation B

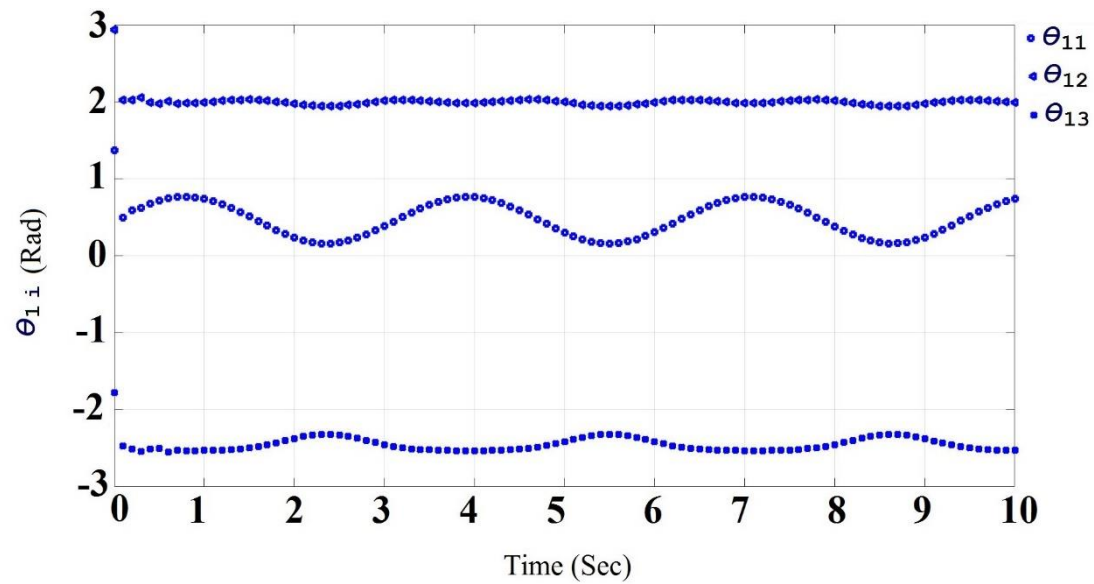


Figure 18 (g). Set 2, simulation C

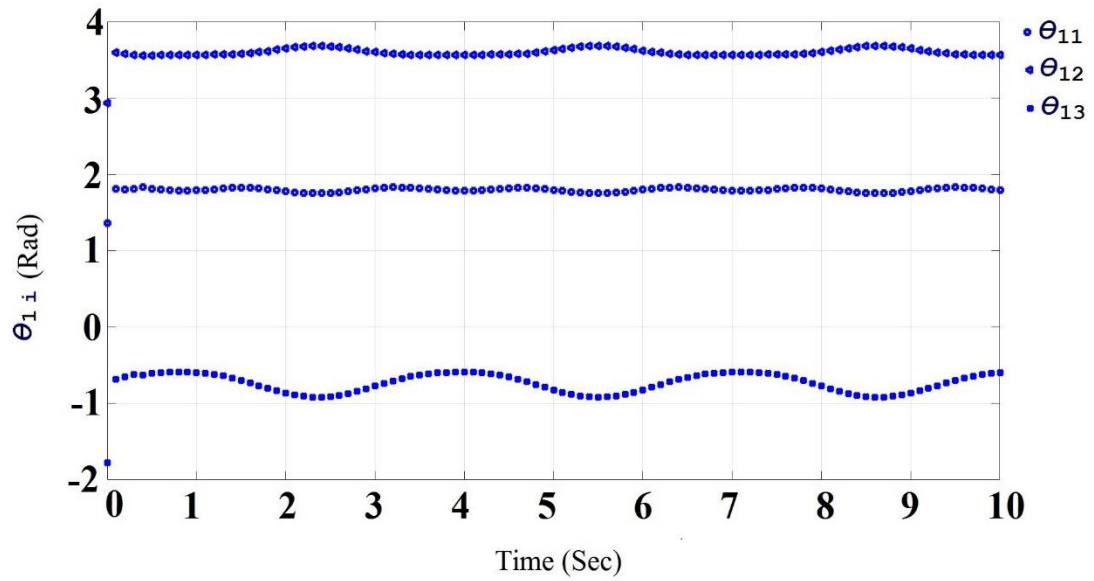


Figure 18 (h). Set 2, simulation D

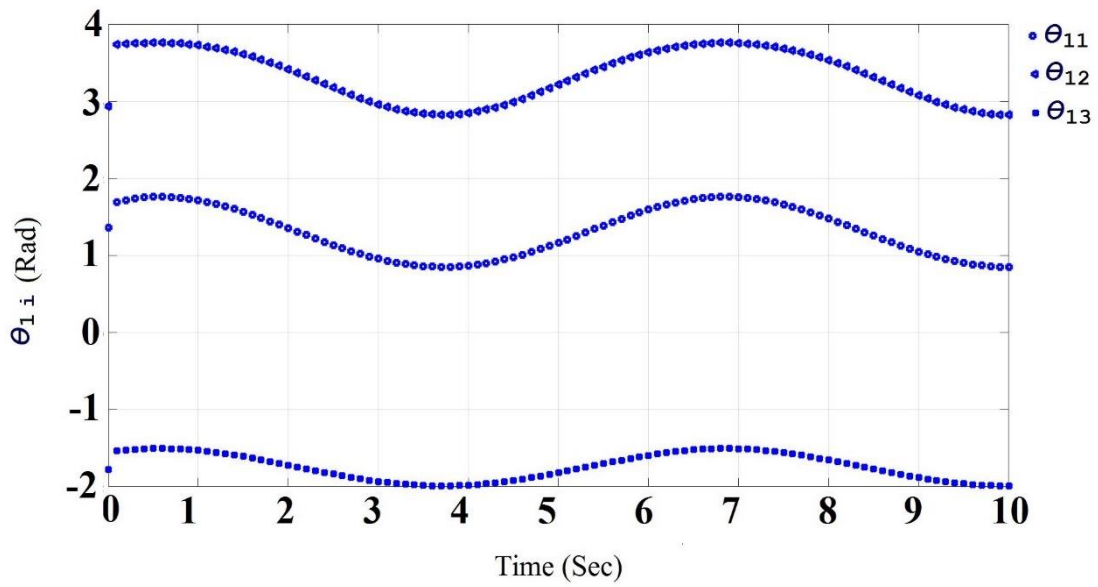


Figure 18 (i). Set 3, simulation A

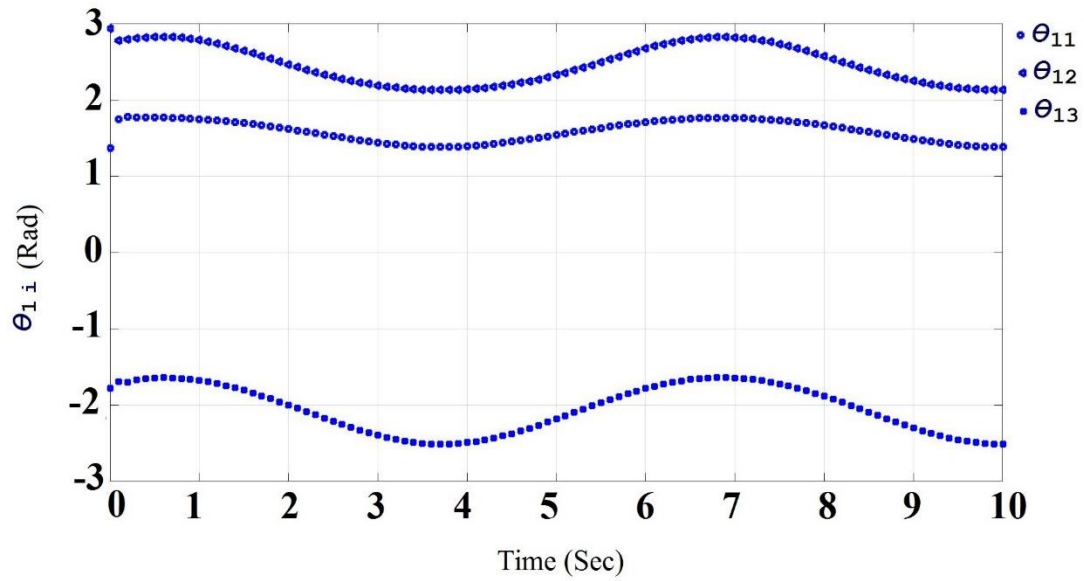


Figure 18 (j). Set 3, simulation B

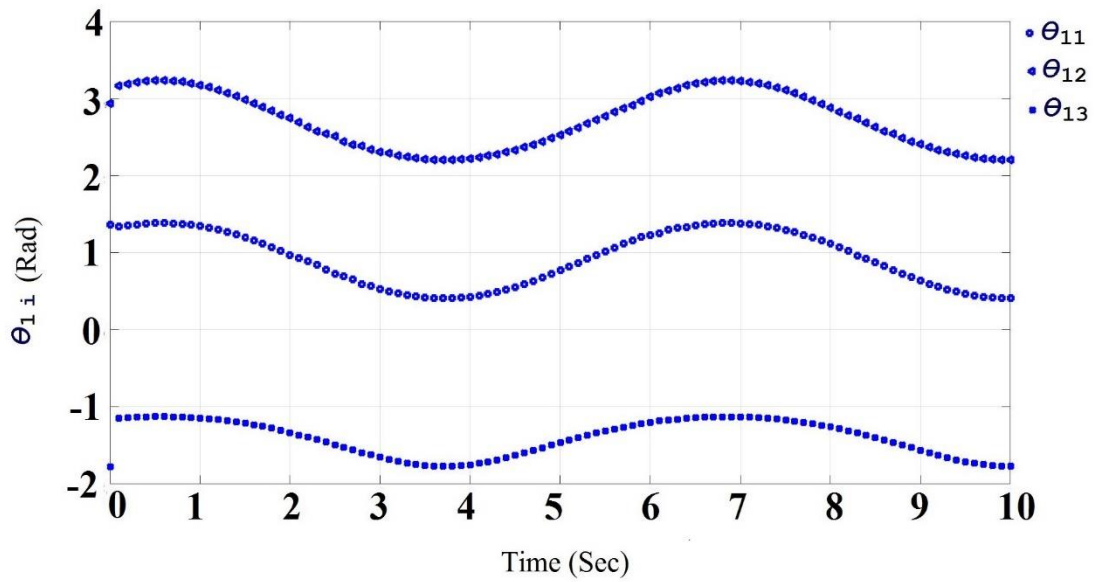


Figure 18 (k). Set 3, simulation C

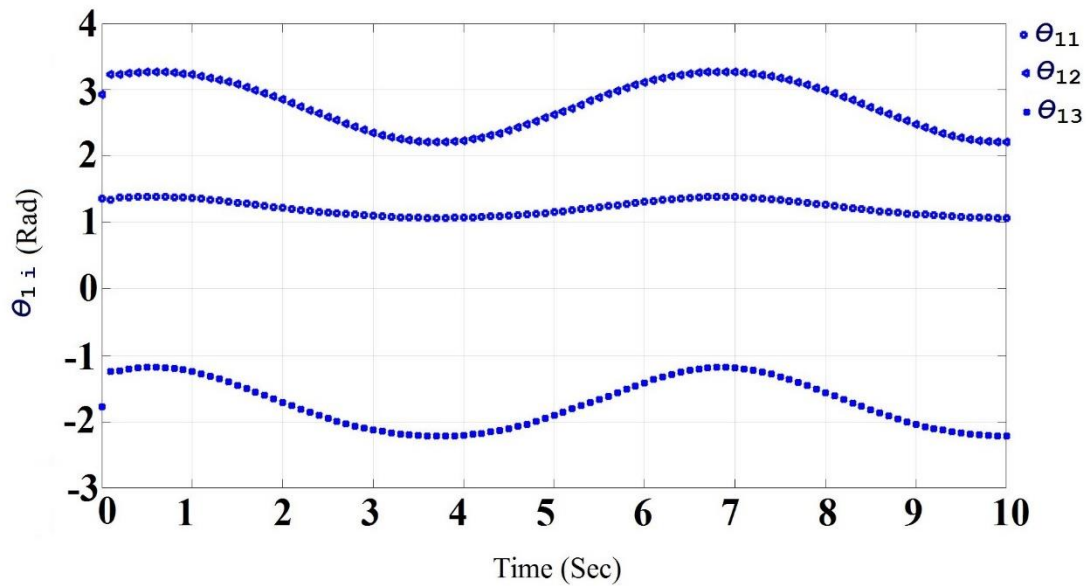


Figure 18 (1). Set 3, simulation D

6.2. Simulations of Lower Part

In the tests for planar part it is checked whether manipulator provide the translational and rotational motions in the desired planar workspace. Behaviors of five active joints are examined with specified movements by using workspace boundaries which were originated from spherical part. This part is also modelled in MATLAB. The same procedure was followed as in the spherical part. Motion control of the manipulator is done by using PID blocks. PID blocks are tuned for first three active joints and fourth and fifth joint separately and these obtained P, I and D values were used (for first three active joints $P = 1.35$, $I = 0.95$ and $D = 0.31$, for fourth active joint $P = 37.05$, $I = 21.62$ and $D = 14.11$ and for fifth active joint $P = 59,59$, $I = 331.09$ and $D = 2.38$). Five different test results can be viewed as followed figures. Table 9 shows that the input variables of the manipulator for three different sets of simulations and figure 19 shows these simulation results. The obtained simulation results show that the dimensional parameters obtained with firefly algorithm provide the workspace completely and the manipulator operated without any singularity condition for planar part.

Table 9. Simulations on planar part

Set 1				
ϕ_1	ϕ_2	ϕ_3	P_x	P_y
Sin Wave	Sin Wave	Sin Wave	Linear	Linear
Amplitude: 0.5	Amplitude: 0.5	Amplitude: 0.5	$P_x = 0, t = (0,300)$	$P_x = 0, t = (0,300)$
F:0.1 rad/sec	F:0.1 rad/sec	F:0.1 rad/sec		
Set 2				
ϕ_1	ϕ_2	ϕ_3	P_x	P_y
Sin Wave	Sin Wave	Sin Wave	Linear	Linear
Amplitude: 0.5	Amplitude: 0.5	Amplitude: 0.5	$P_x = 8t, t = (0,150)$ $P_x = 120, t = (150,300)$	$P_y = -8t, t = (0,150)$ $P_x = -120, t = (120,300)$
F:0.1 rad/sec	F:0.1 rad/sec	F:0.1 rad/sec		
Set 3				
ϕ_1	ϕ_2	ϕ_3	P_x	P_y
Sin Wave	Sin Wave	Sin Wave	Linear	Linear
Amplitude: 0.5	Amplitude: 0.5	Amplitude: 0.5	$P_x = 8t, t = (0,150)$ $P_x = 120, t = (150,300)$	$P_y = 8t, t = (0,150)$ $P_y = 120, t = (150,300)$
F:0.1 rad/sec	F:0.1 rad/sec	F:0.1 rad/sec		
Set 4				
ϕ_1	ϕ_2	ϕ_3	P_x	P_y
Sin Wave	Sin Wave	Sin Wave	Linear	Linear
Amplitude: 0.5	Amplitude: 0.5	Amplitude: 0.5	$P_x = -8t, t = (0,150)$ $P_x = -120, t = (150,300)$	$P_x = -8t, t = (0,150)$ $P_x = -120, t = (150,300)$
F:0.1 rad/sec	F:0.1 rad/sec	F:0.1 rad/sec		
Set 5				
ϕ_1	ϕ_2	ϕ_3	P_x	P_y
Sin Wave	Sin Wave	Sin Wave	Linear	Linear
Amplitude: 0.5	Amplitude: 0.5	Amplitude: 0.5	$P_x = -8t, t = (0,150)$ $P_x = -120, t = (150,300)$	$P_x = 8t, t = (0,150)$ $P_x = 120, t = (150,300)$
F:0.1 rad/sec	F:0.1 rad/sec	F:0.1 rad/sec		

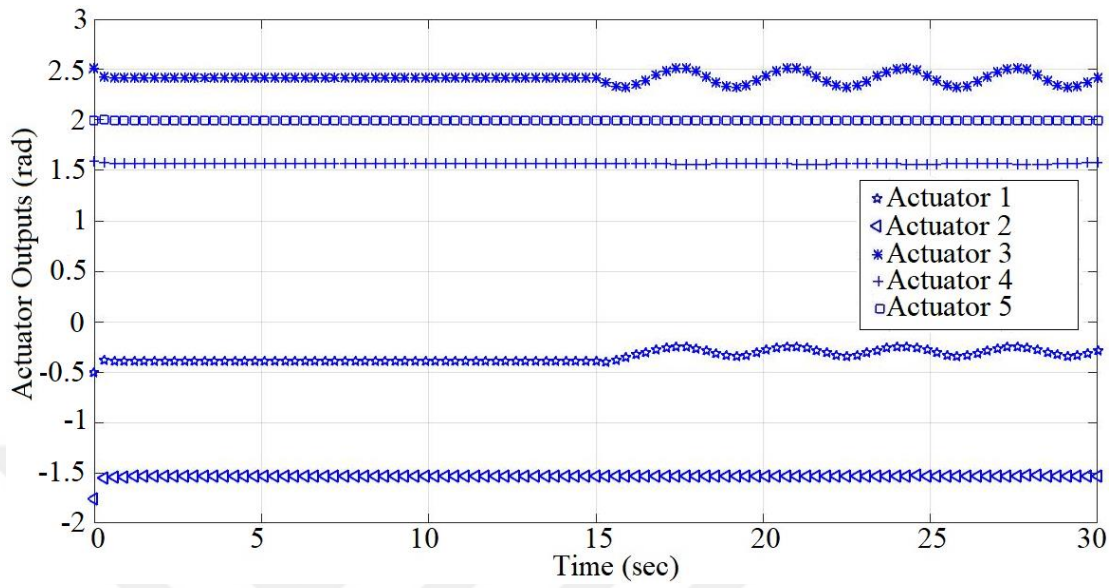


Figure 19 (a). Test results for planar part optimization (Set 1)

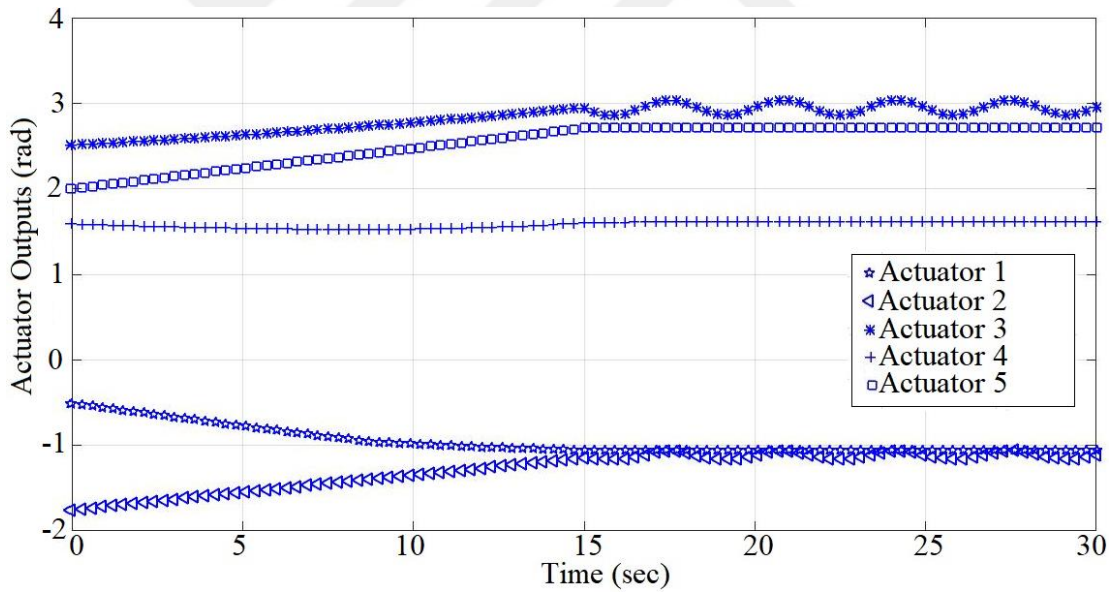


Figure 19 (b). Test results for planar part optimization (Set 2)

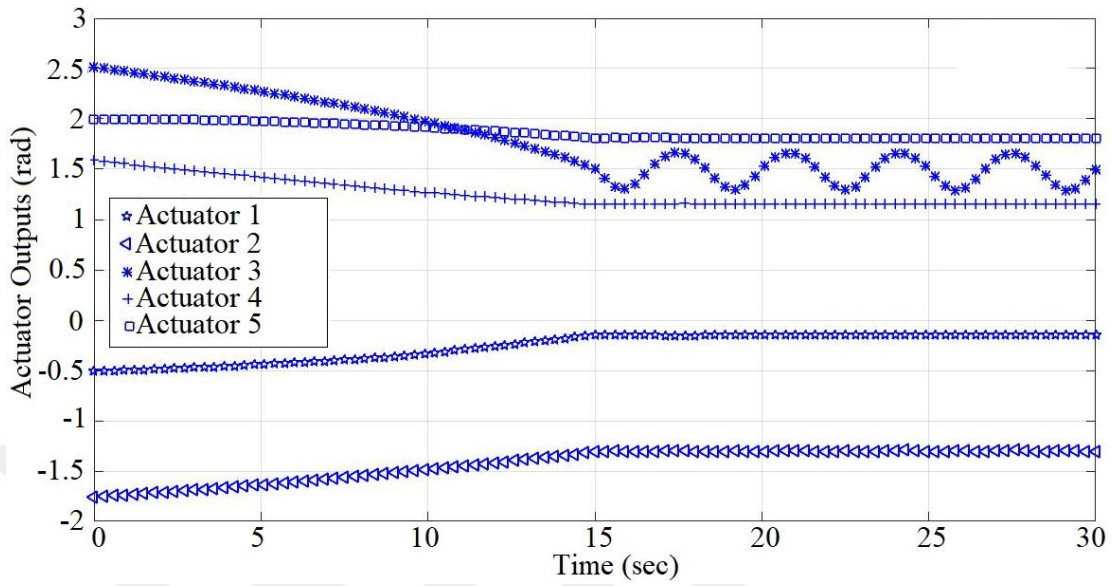


Figure 19 (c). Test results for planar part optimization (Set 3)

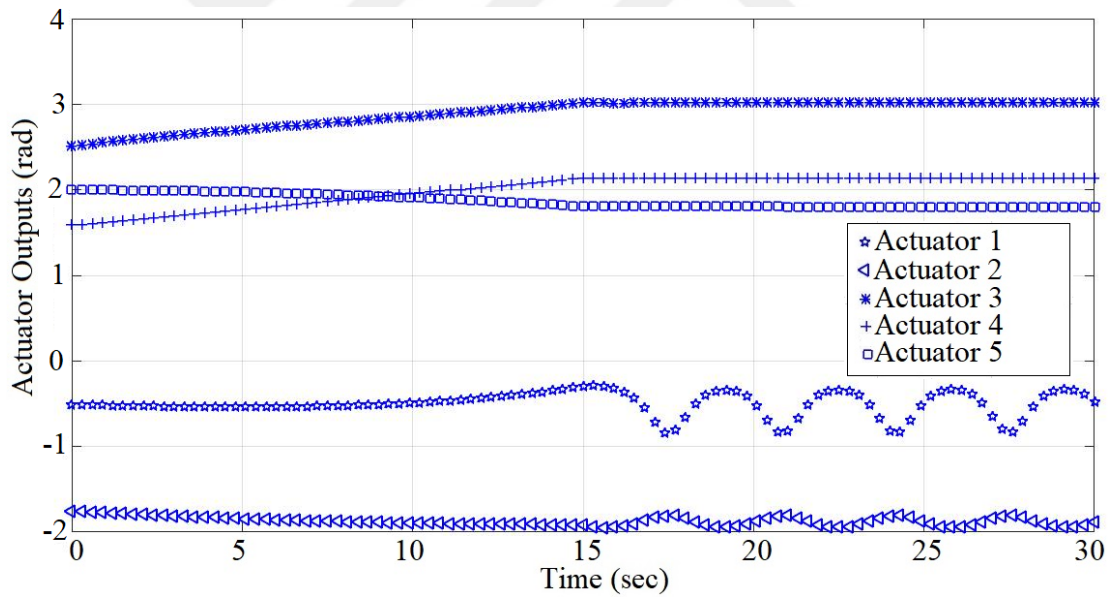


Figure 19 (d). Test results for planar part optimization (Set 4)

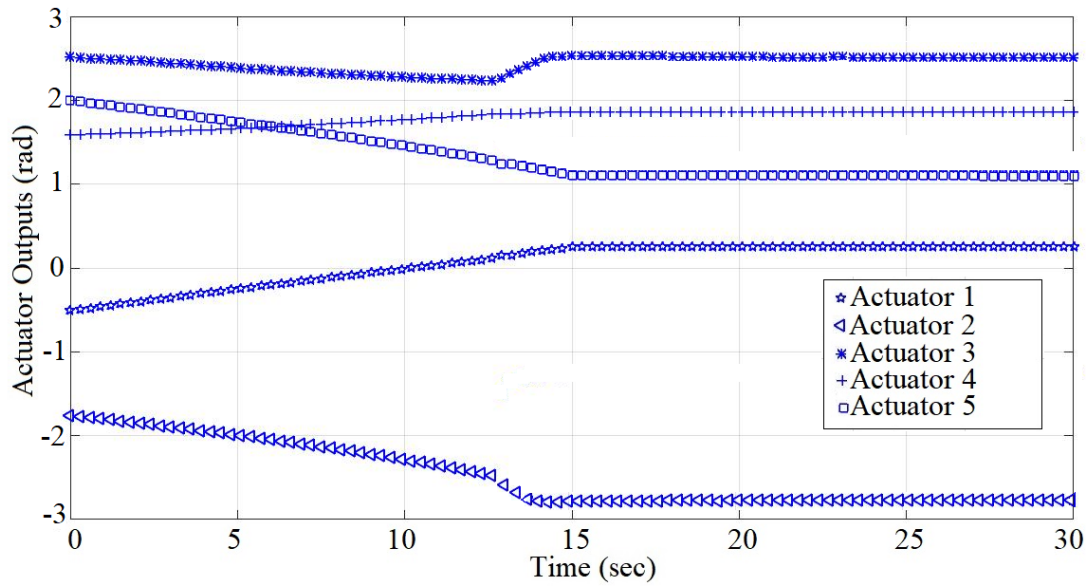


Figure 19 (e). Test results for planar part optimization (Set 5)

6.3. Simulations of Whole Manipulator

In the tests for whole manipulator it is checked whether manipulator provide the translational and rotational motions in the desired workspace. Behaviors of five active joints are examined with specified movements by using workspace boundaries which were originated from both spherical and planar part. Whole manipulator is also modelled in MATLAB. Motion control of the manipulator is done by using PID blocks. The same procedure was followed as in the both spherical and planar parts. PID blocks are tuned for first three active joints and fourth and fifth joint separately and these obtained P, I and D values were used (for first three active joints $P = 1.35$, $I = 0.95$ and $D = 0.31$, for fourth active joint $P = 37.05$, $I = 21.62$ and $D = 14.11$ and for fifth active joint $P = 59,59$, $I = 331.09$ and $D = 2.38$). Fifteen different test results can be viewed as followed figures. Table 10 shows that the input variables of the manipulator for fifteen different sets of simulations and figure 20 shows these simulation results. The obtained simulation results show that the dimensional parameters obtained with firefly algorithm provide the workspace completely and the manipulator operated without any singularity condition within given workspace completely. Simmechanics model of spherical, planar and whole manipulator are given in appendix A.

Table 10. Simulations on whole manipulators

Note: Rotational motions are applied at time interval between 150 and 300 seconds.

Set 1				
δ_1	δ_2	δ_3	P_x	P_y
Sin Wave	Constant	Constant	Constant	Constant
Amplitude: 0.4	Magnitude: 0	Magnitude: 0	Magnitude: 0	Magnitude: 0
F:0.1 rad/sec				
Set 2				
δ_1	δ_2	δ_3	P_x	P_y
Constant	Sin Wave	Constant	Constant	Constant
Magnitude: 0	Amplitude: 0.5	Magnitude: 0	Magnitude: 0	Magnitude: 0
F:0.1 rad/sec				
Set 3				
δ_1	δ_2	δ_3	P_x	P_y
Constant	Constant	Sin Wave	Constant	Constant
Magnitude: 0	Magnitude: 0	Amplitude: 0.6	Magnitude: 0	Magnitude: 0
F:0.1 rad/sec				
Set 4				
δ_1	δ_2	δ_3	P_x	P_y
Sin Wave	Constant	Constant	Linear	Linear
Amplitude: 0.4	Magnitude: 0	Magnitude: 0	$P_x = 8t, t = (0,150)$ $P_y = -8t, t = (0,150)$	$P_x = 120, t = (150,300)$ $P_y = -120, t = (150,300)$
F:0.1 rad/sec				
Set 5				
δ_1	δ_2	δ_3	P_x	P_y
Sin Wave	Sin Wave	Sin Wave	Linear	Linear
Magnitude: 0	Amplitude: 0.5	Magnitude: 0	$P_x = 8t, t = (0,150)$ $P_y = -8t, t = (0,150)$	$P_x = 120, t = (150,300)$ $P_y = -120, t = (150,300)$
F:0.1 rad/sec				
Set 6				
δ_1	δ_2	δ_3	P_x	P_y
Constant	Constant	Sin Wave	Linear	Linear
Magnitude: 0	Magnitude: 0	Amplitude: 0.6	$P_x = 8t, t = (0,150)$ $P_y = -8t, t = (0,150)$	$P_x = 120, t = (150,300)$ $P_y = -120, t = (150,300)$
F:0.1 rad/sec				
Set 7				
δ_1	δ_2	δ_3	P_x	P_y
Sin Wave	Constant	Constant	Linear	Linear
Amplitude: 0.4	Magnitude: 0	Magnitude: 0	$P_x = 8t, t = (0,150)$ $P_y = 8t, t = (0,150)$	$P_x = 120, t = (150,300)$ $P_y = 120, t = (150,300)$

F:0.1 rad/sec	F:0.1 rad/sec	F:0.1 rad/sec		
Set 8				
δ_1	δ_2	δ_3	P_x	P_y
Sin Wave	Sin Wave	Sin Wave	Linear	Linear
Magnitude: 0	Amplitude: 0.5	Magnitude: 0	$P_x = 8t, t = (0,150)$ $P_y = 8t, t = (0,150)$	$P_x = 120, t = (150,300)$ $P_y = 120, t = (150,300)$
F:0.1 rad/sec				
Set 9				
δ_1	δ_2	δ_3	P_x	P_y
Constant	Constant	Sin Wave	Linear	Linear
Magnitude: 0	Magnitude: 0	Amplitude: 0.6	$P_x = 8t, t = (0,150)$ $P_y = 8t, t = (0,150)$	$P_x = 120, t = (150,300)$ $P_y = 120, t = (150,300)$
F:0.1 rad/sec				
Set 10				
δ_1	δ_2	δ_3	P_x	P_y
Sin Wave	Constant	Constant	Linear	Linear
Amplitude: 0.4	Magnitude: 0	Magnitude: 0	$P_x = -8t, t = (0,150)$ $P_y = -8t, t = (0,150)$	$P_x = -120, t = (150,300)$ $P_y = -120, t = (150,300)$
F:0.1 rad/sec				
Set 11				
δ_1	δ_2	δ_3	P_x	P_y
Sin Wave	Sin Wave	Sin Wave	Linear	Linear
Magnitude: 0	Amplitude: 0.5	Magnitude: 0	$P_x = -8t, t = (0,150)$ $P_y = -8t, t = (0,150)$	$P_x = -120, t = (150,300)$ $P_y = -120, t = (150,300)$
F:0.1 rad/sec				
Set 12				
δ_1	δ_2	δ_3	P_x	P_y
Constant	Constant	Sin Wave	Linear	Linear
Magnitude: 0	Magnitude: 0	Amplitude: 0.6	$P_x = -8t, t = (0,150)$ $P_y = -8t, t = (0,150)$	$P_x = -120, t = (150,300)$ $P_y = -120, t = (150,300)$
F:0.1 rad/sec				
Set 13				
δ_1	δ_2	δ_3	P_x	P_y
Sin Wave	Constant	Constant	Linear	Linear
Amplitude: 0.4	Magnitude: 0	Magnitude: 0	$P_x = -8t, t = (0,150)$ $P_y = 8t, t = (0,150)$	$P_x = -120, t = (150,300)$ $P_y = 120, t = (150,300)$
F:0.1 rad/sec				
Set 14				
δ_1	δ_2	δ_3	P_x	P_y
Sin Wave	Sin Wave	Sin Wave	Linear	Linear

Magnitude: 0	Amplitude: 0.5	Magnitude: 0	$P_x = -8t, t = (0,150)$ $P_y = 8t, t = (0,150)$	$P_x = -120, t = (150,300)$ $P_y = 120, t = (150,300)$
F:0.1 rad/sec				

Set 15				
δ_1	δ_2	δ_3	P_x	P_y
Constant	Constant	Sin Wave	Linear	Linear
Magnitude: 0	Magnitude: 0	Amplitude: 0.6	$P_x = -8t, t = (0,150)$ $P_y = 8t, t = (0,150)$	$P_x = -120, t = (150,300)$ $P_y = 120, t = (150,300)$
F:0.1 rad/sec				

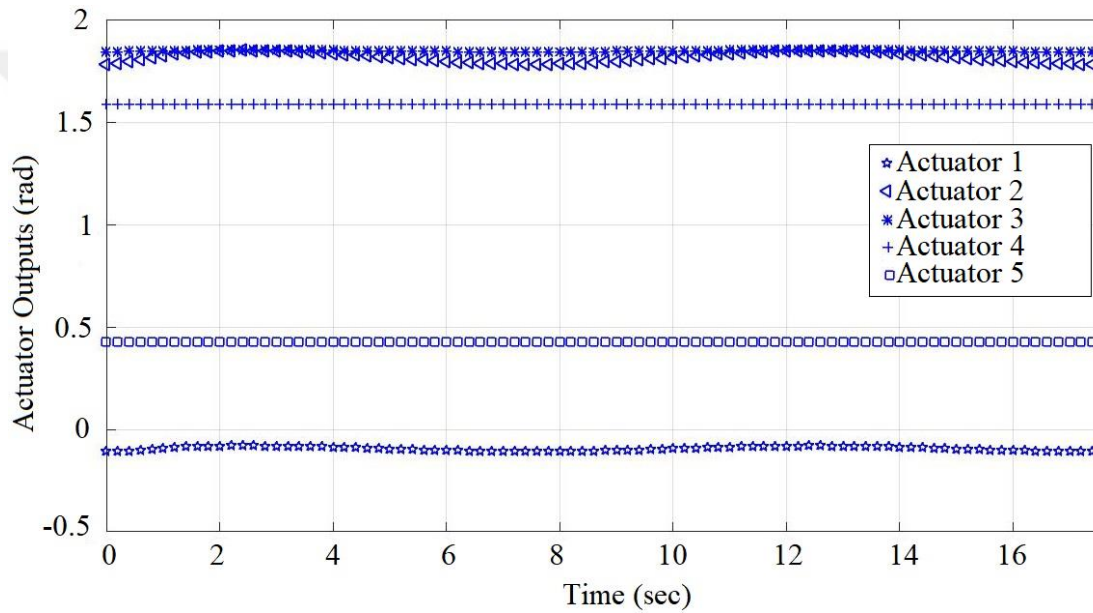


Figure 20 (a). Test results for whole part manipulator (Set 1)

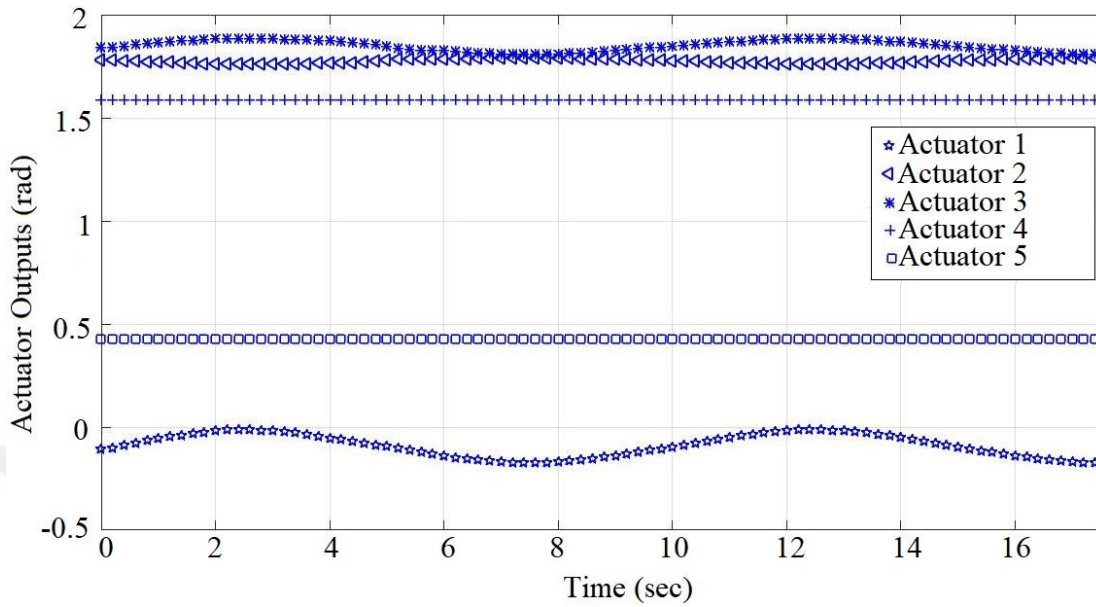


Figure 20 (b). Test results for whole part manipulator (Set 2)

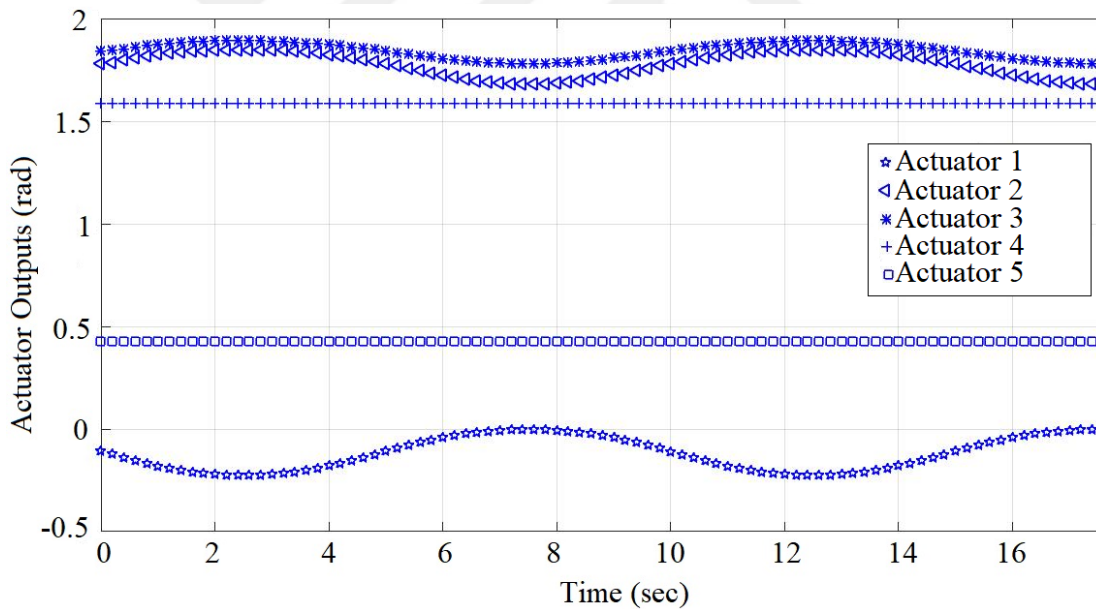


Figure 20 (c). Test results for whole part manipulator (Set 3)

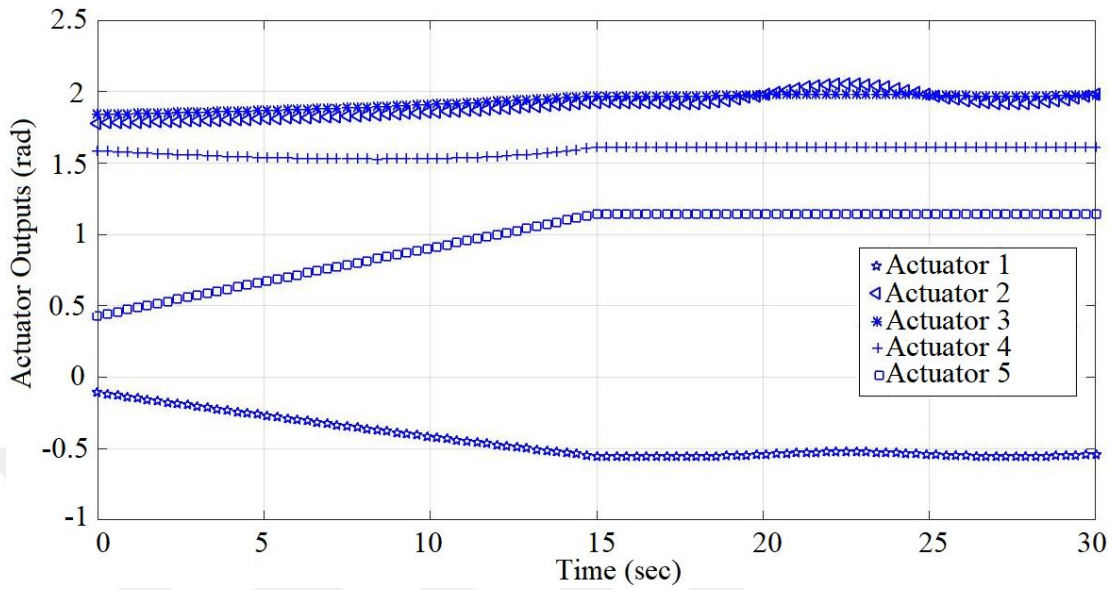


Figure 20 (d). Test results for whole part manipulator (Set 4)

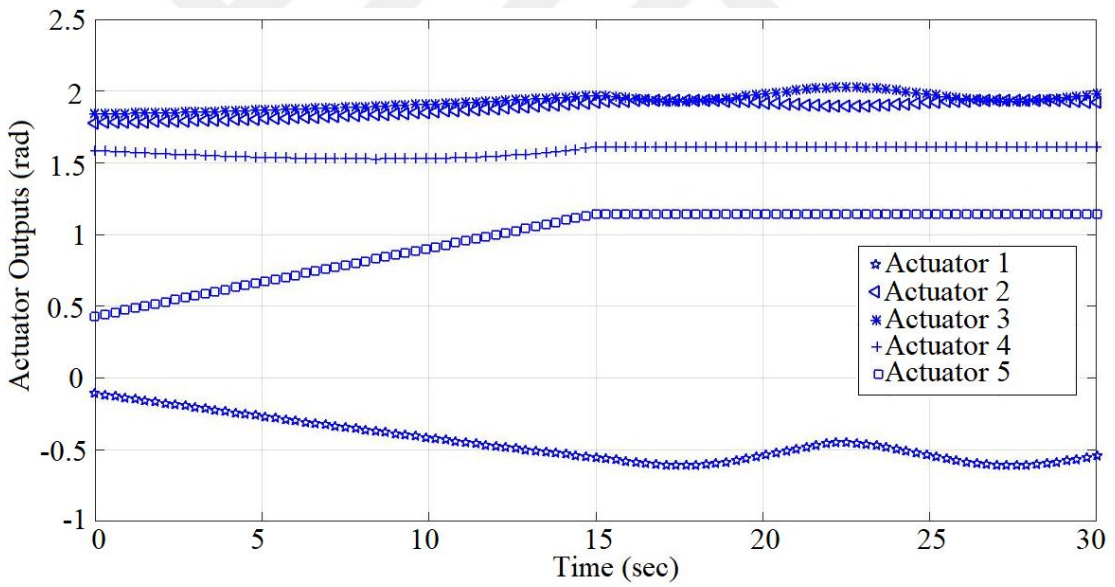


Figure 20 (e). Test results for whole part manipulator (Set 5)

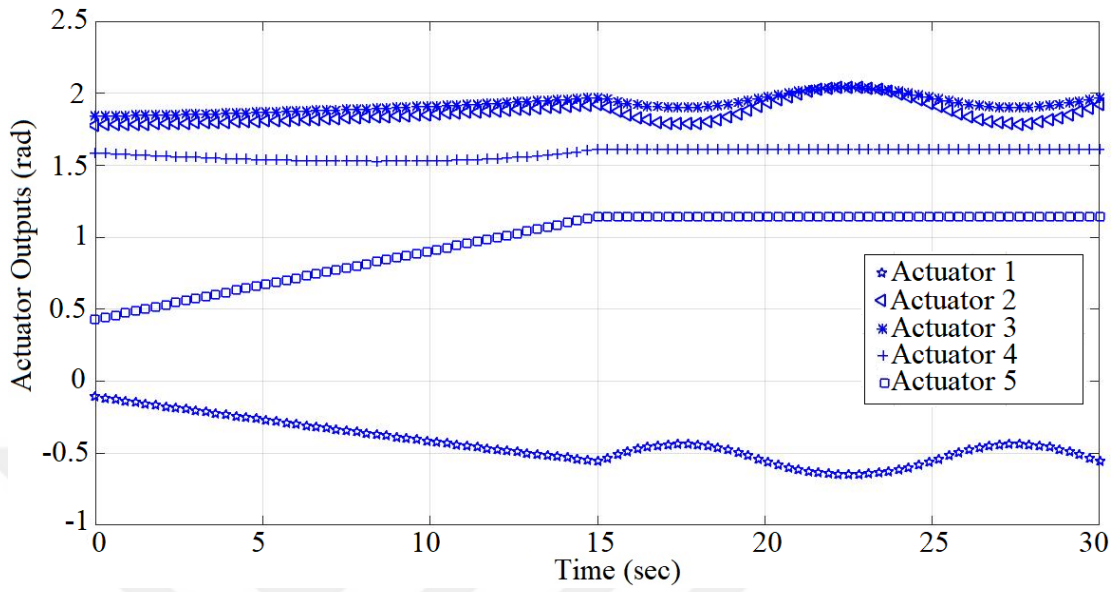


Figure 20 (f). Test results for whole part manipulator (Set 6)

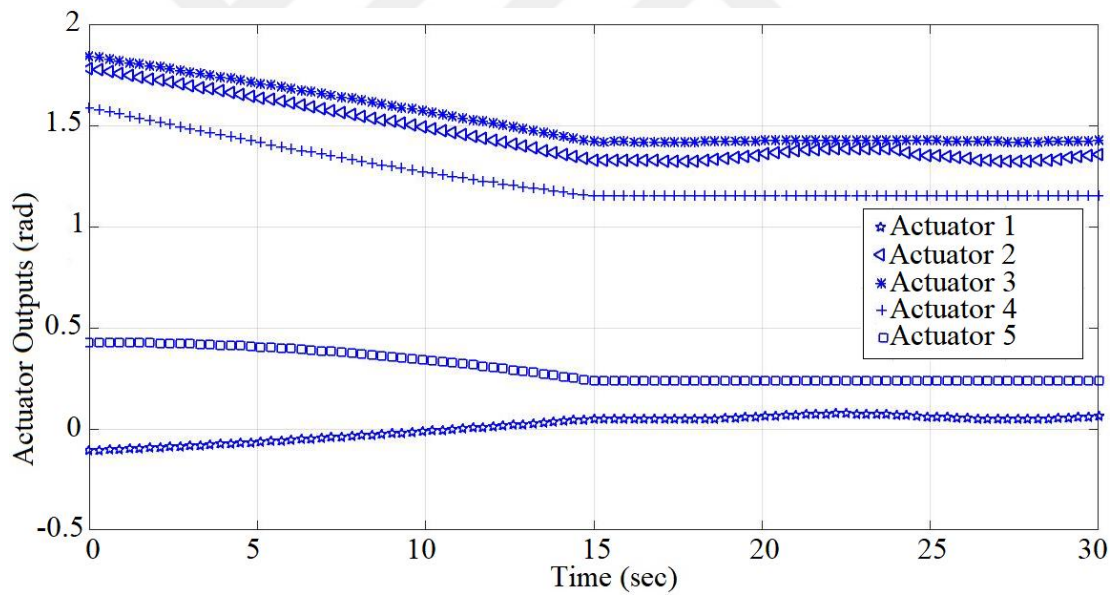


Figure 20 (g). Test results for whole part manipulator (Set 7)

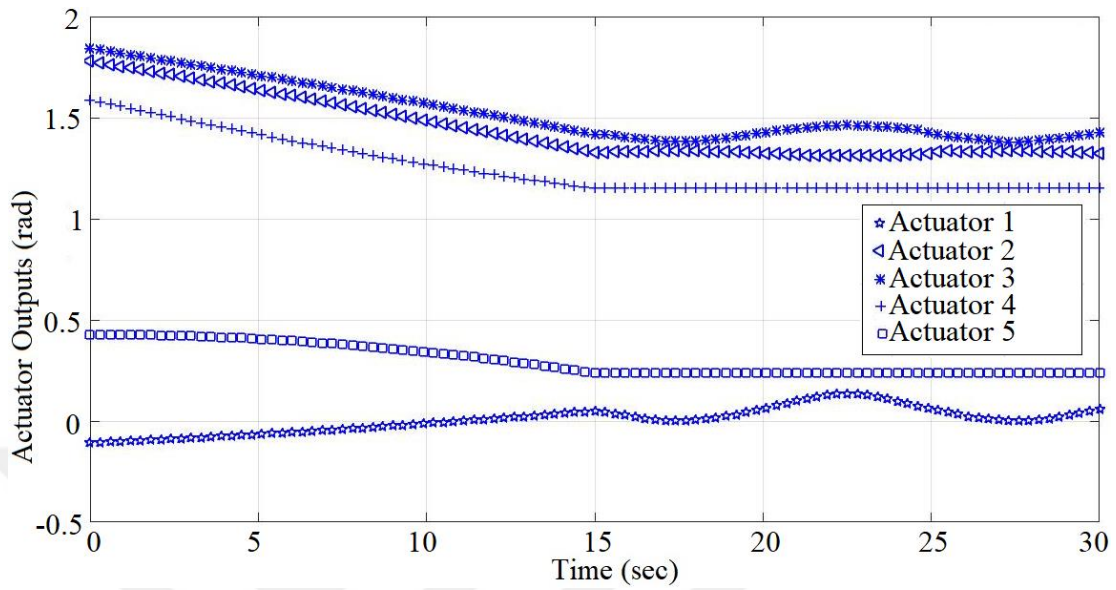


Figure 20 (h). Test results for whole part manipulator (Set 8)

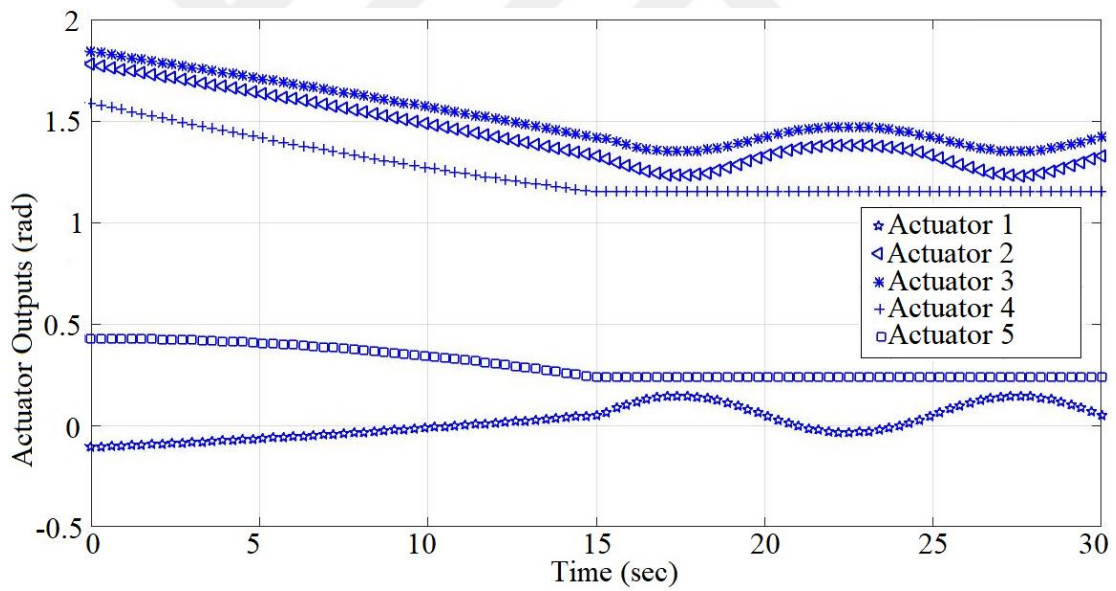


Figure 20 (i). Test results for whole part manipulator (Set 9)

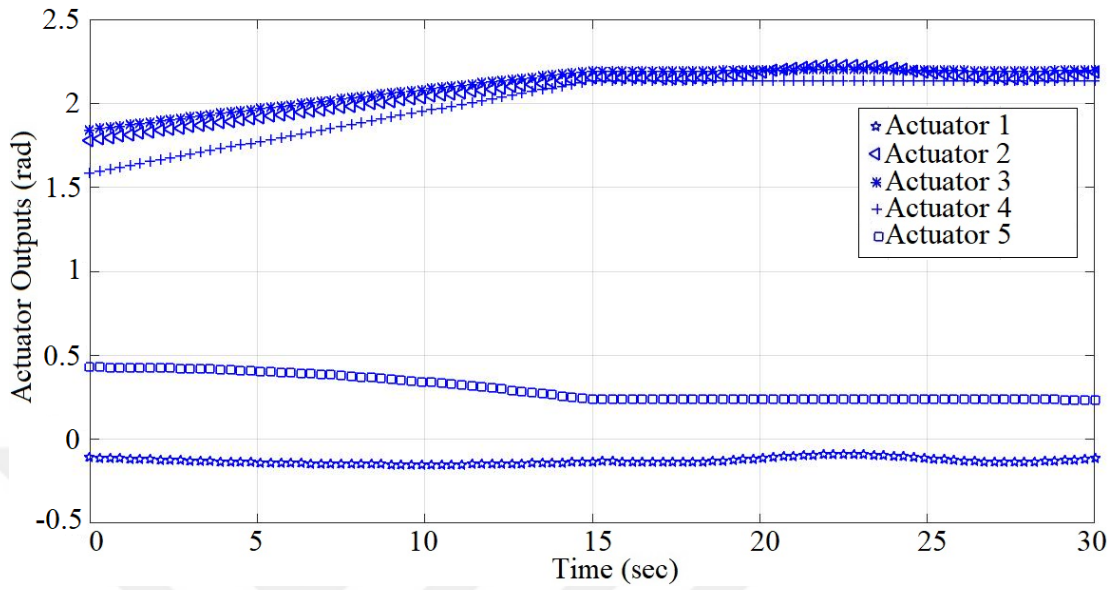


Figure 20 (j). Test results for whole part manipulator (Set 10)

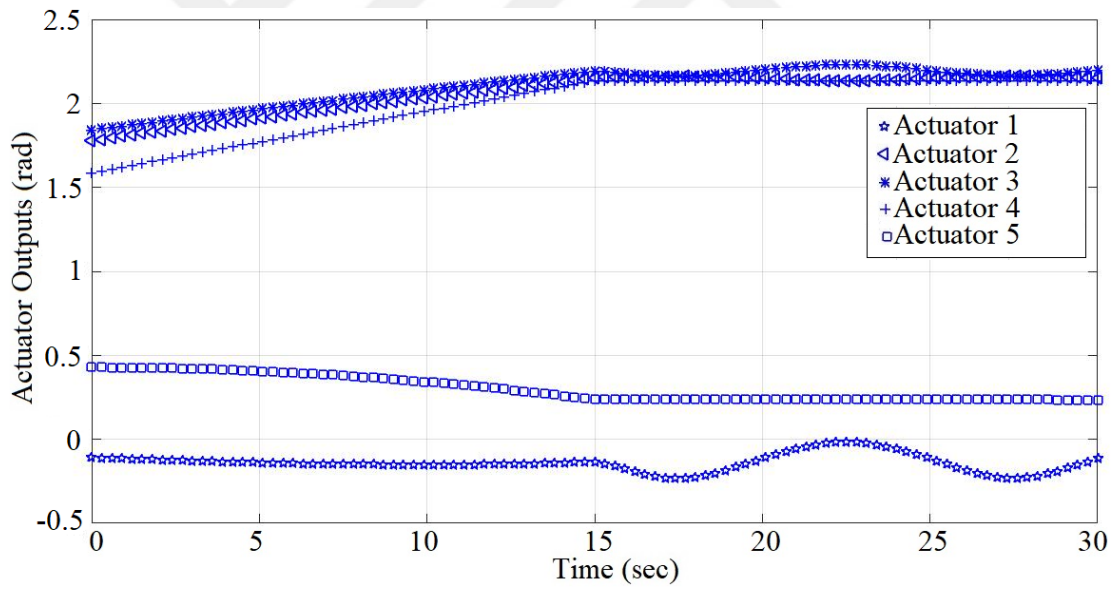


Figure 20 (k). Test results for whole part manipulator (Set 11)

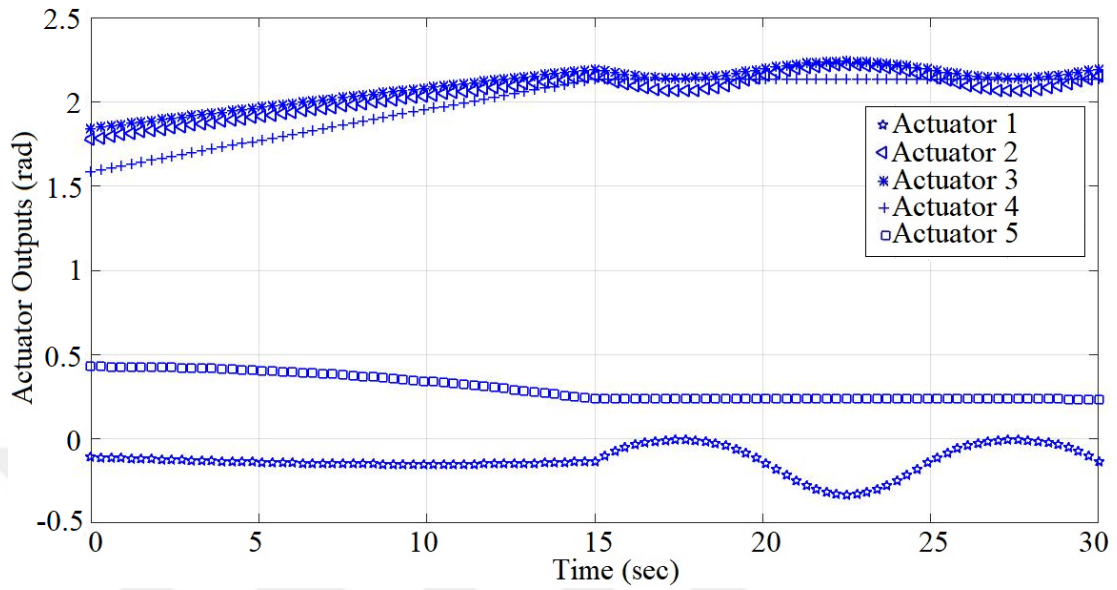


Figure 20 (l). Test results for whole part manipulator (Set 12)

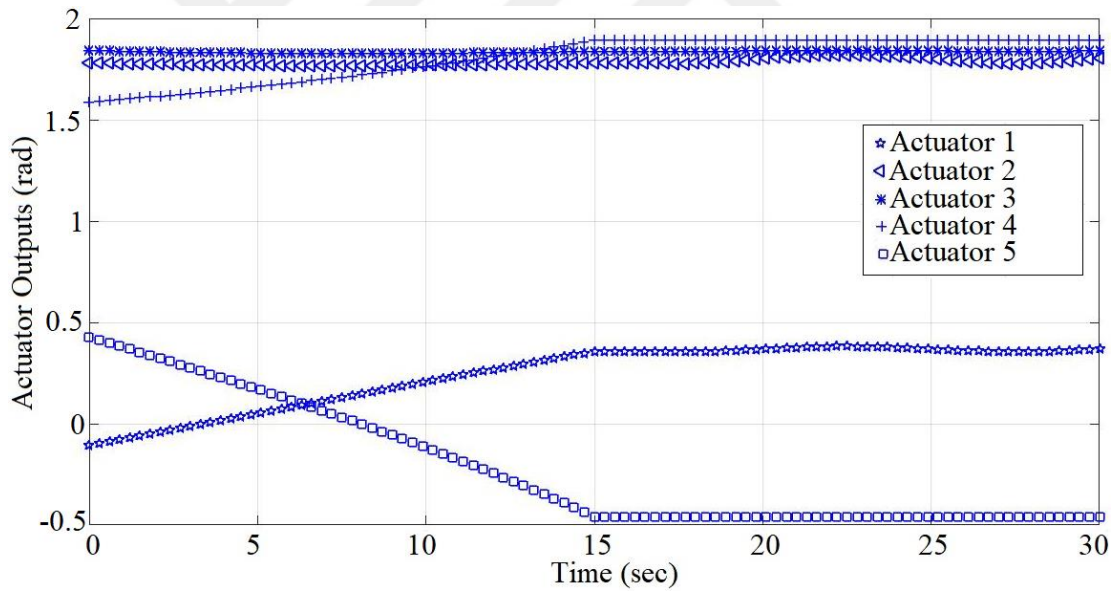


Figure 20 (m). Test results for whole part manipulator (Set 13)

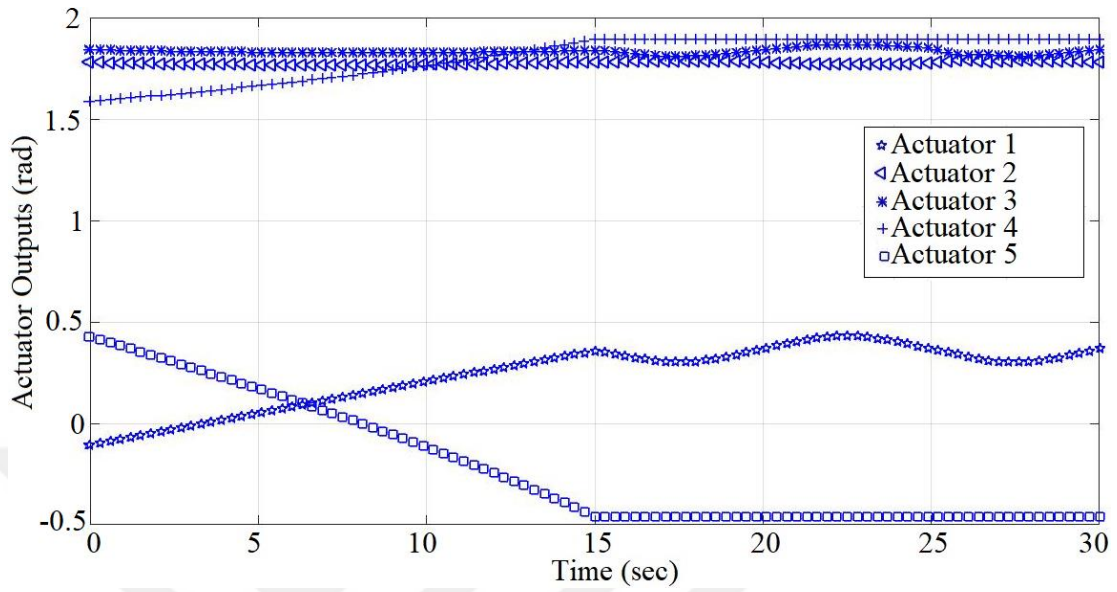


Figure 20 (n). Test results for whole part manipulator (Set 14)

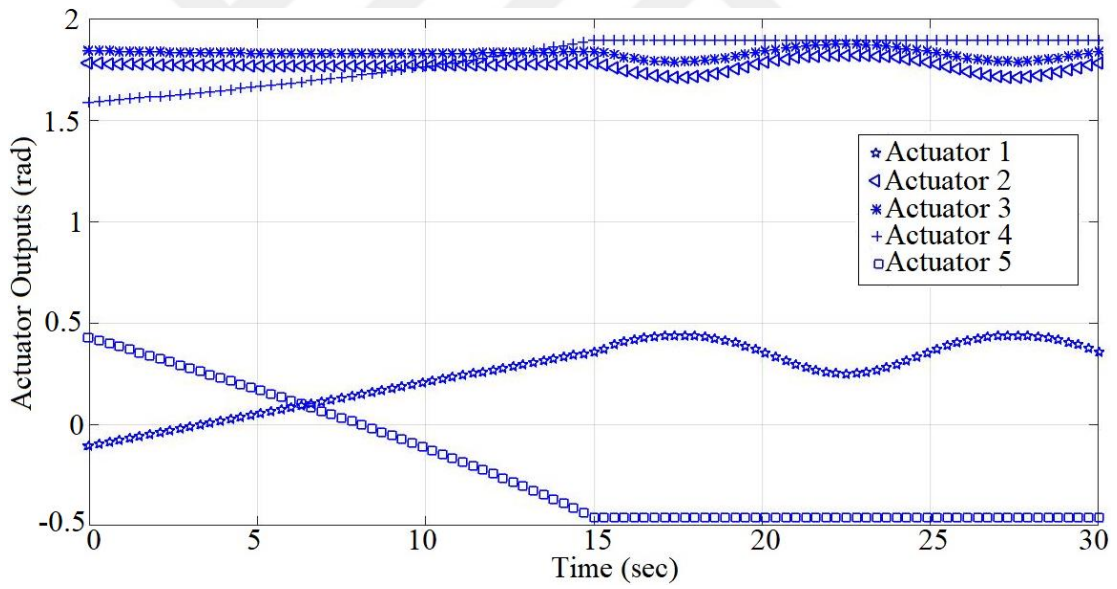


Figure 20 (o). Test results for whole part manipulator (Set 15)

7. FORCE ANALYSIS OF MANIPULATOR

Force analysis plays important role on rehabilitation robotics because of these kind of robots directly interact with human bodies. To avoid harmful situations, forces acting on the manipulator from environment and users to manipulator and from manipulator to human should be predictable. After dynamic analysis we could select required actuators to use for the manipulator. Multiple closed loops lead to complication of dynamic solution of parallel manipulators [1]. The main approaches could be used to solve dynamic equations of any parallel manipulators. These approaches can be listed as; Newton-Euler formulation, the Lagrangian formulation and the principle of virtual work. The designed manipulator is a parallel manipulator and it is considered that when the manipulator's end effector moves from one location to another, it moves slowly (near a constant speed). So there is low acceleration. Also, the weight effect of the manipulator is less than the external forces. In such cases, we can use static calculations to get a relation for external forces and actuator torques. Jacobian matrix analysis can help us to define force relations between actuators and environment. We defined Jacobian relation for spherical part in chapter 4. We can define it for force relation as follow.

$$J_{S_x} \mathbf{M} = J_{S_q} \boldsymbol{\tau}_S \quad (65)$$

Here \mathbf{M} refers to external moments from all direction (3x1 matrix vector) and its components becomes $\mathbf{M}_x, \mathbf{M}_y$ and \mathbf{M}_z respectively. $\boldsymbol{\tau}_S$ refers imaginary active joint torques and its components becomes $\boldsymbol{\tau}_{S,1}, \boldsymbol{\tau}_{S,2}$ and $\boldsymbol{\tau}_{S,3}$ respectively. We can express $\boldsymbol{\tau}_S$ with following relation.

$$\boldsymbol{\tau}_S = J_{S_q}^{-1} J_{S_x} \mathbf{M} \quad (66)$$

These calculated torque values for spherical part become external moment components for planar part. Besides that, two external forces are acting on planar sub-manipulator in direction x and y. With considering these external forces, we can write down force relation for planar part as following equation.

$$J_{p_x} \mathbf{E}_E = J_{p_q} \boldsymbol{\tau}_p \quad (67)$$

Now here, \mathbf{E}_E refers external effects acting on planar sub-manipulator. Finally, we can compute needed torque values actuator as following equation.

$$\boldsymbol{\tau}_p = J_{p_q}^{-1} J_{p_x} \mathbf{E}_E \quad (68)$$

In static force analysis, external moments are selected 1 N.m for wrist torque [47] around three different axes. From Eq. 66, torques of imaginary active joints are found -0.17 N.m, -1.66 N.m and -1.96 N.m respectively. These values are used for lower sub-system. Also, external forces on x and y directions are selected as 10 N.

From Eq. 68, motor torques are found -3.63 N.m, 3.37 N.m, 2.41 N.m, -11.16 N.m and 6.28 N.m respectively.



8. CONCLUSION

This thesis deals with the design, analysis and dimensional optimization of 5 DoFs over-constrained planar-spherical parallel manipulator. This manipulator is designed to improve the efficiency of treatment of human shoulder, elbow and wrist and help the patients to daily living activities faster. Since the subspace of the manipulator match up with the subspace between the shoulder, elbow and wrist, this kind of a design are selected. Because of this mechanism has specific spatial workspace boundaries, could be used for special cases.

Every design begins with determining how and where the design will be used. So, we started to design with specification of the motion of manipulator during rehabilitation. We consider a sphere which can perform three rotational motions around x, y and z axes and two translational motions on x and y axes. This motion set has subspace number five. For five independent movements five actuators are needed. After specification of degrees of freedom, leg and joint numbers are selected.

Next step is the determination of the geometry of the manipulator. Remember, we have both planar motion in plane and rotational motion in space. So, our manipulator should have both planar and spherical parts. A three degrees of freedom spherical manipulator can provide three rotational motions around three different axes. Of course, a two degrees of freedom manipulator can perform a plane motion on two different axes. Because of we have parallel manipulator, we should place all actuators at ground joints or near the ground joints. Placing one actuator at first three legs will provide the spherical motion and placing last two actuators to fourth leg will provide the planar motion.

Before optimization processes are performed for the manipulator, we obtained constraints and objective function by doing inverse kinematic and Jacobian analysis. Optimization processes are performed by using Firefly Algorithm. Firefly Algorithm is a nature inspired metaheuristic algorithm which is very effective for optimization task in several different ways.

After optimized dimensional parameters are obtained, the manipulator is tested in given workspace boundaries by simulated with using MATLAB. Several simulations are done for several different cases. The obtained simulation results show that the dimensional parameters obtained with Firefly Algorithm provide the definite workspace completely and the manipulator is operated without any singularity condition both spherical and planar parts.

Static force relations are established for both spherical and planar part of the manipulator. Selection of 4 N.m motor torque for first three actuators, 12 N.m motor torque for fourth actuator and 8 N.m motor torque for fifth actuator will be sufficient to drive manipulator.

In this thesis, a 5 DOFs parallel over-constrained manipulator was proposed for rehabilitation purpose. Its workspace was defined and manipulator geometry was given. After that, inverse kinematic solution of the manipulator was done and Jacobian analysis of the manipulator was proposed. Then, dimensional parameters of the manipulator were found by using Firefly algorithm. Several simulations were done for spherical, planar and whole manipulator and it was seen that founded dimensional parameters were fulfill the proposed workspace without any singularity condition.

REFERENCES

1. Tsai L. W. (1999), "*Robot Analysis: The Mechanics of Serial and Parallel Manipulators*", John Wiley and Sons, INC.
2. Ghosal A. (2006), "*Kinematics of Serial Manipulators*"
3. Özgören K. (2015), "*Seri ve Paralel Manipulatorlerin Analitik ve Yarı-Analitik Yöntemlerle Konum ve Hız Analizleri*", Ders Notları Serisi -1, Makine Teorisi Derneği
4. Tanev T. K. (1999), "*Kinematics of a hybrid (parallel – serial) robot manipulators*", Mechanism and Machine Theory 35 (2000) pp. 1183-1196
5. Nanua P., Waldron K. J., Murthy V. (1990), "*Direct Kinematic Solution of a Stewart Platform*", IEEE Transaction on Robotics and Automation, vol. 6, no. 4.
6. What is a parallel robot? Retrieved from: <http://www.mecademic.com/What-is-a-parallel-robot.html> (Last Access: 10.04.2017, 11:00)
7. Pollard W. L. (1942), "*Position Controlling Apparatus*", US Patent No. 2286571, 1942.
8. Gough V. E. and Whitehall S. G. (1962), "*Universal Tyre Test Machine*", Proceedings of 9th International Congress FISITA, May 1962, pp. 117-137
9. Patel, Y. D., George, P.M. (2012), "*Parallel Manipulators Applications – A Survey*" Modern Mechanical Engineering, 2012, 2, pp. 57-64
10. Aldulaimi, H. (2015), "*Design and Analysis of an Overconstrained Manipulator for Rehabilitation*", Master Thesis, Çankaya University, 2015
11. Wrosch, C., Miker, G. E., Scheier, M. F., Pontet, S. B. (2007), "*Giving up on unattainable goals: Benefits for health?*", Personality and Social Psychology Bulletin, 35(2), pp. 251-265
12. Bühler, C. (1998), "*Robotics for Rehabilitation – a European Perspective*", Robotica volume 16, United Kingdom, Cambridge University Press
13. Klein, J., Spencer, S., Allington, J., Bobrow, J. E., & Reinkensmeyer, D. J. (2010), "*Optimization of a parallel shoulder mechanism to achieve a high-force, low-mass, robotic-arm exoskeleton*", IEEE Transactions on Robotics, 26(4), 710-715.

14. Mao, Y., Agrawal, S. K. (2011), “*A cable driven upper arm exoskeleton for upper extremity rehabilitation*”, Robotics and Automation (ICRA), 2011 IEEE International Conference on (pp. 4163-4168). IEEE.
15. O'Malley, M. K., Sledd, A., Gupta, A., Patoglu, V., Huegel, J., Burgar, C. (2006), “*The RiceWrist: A distal upper extremity rehabilitation robot for stroke therapy*”, ASME 2006 International Mechanical Engineering Congress and Exposition (pp. 1437-1446). American Society of Mechanical Engineers.
16. Pehlivan, A. U., Celik, O., O'Malley, M. K. (2011), “*Mechanical design of a distal arm exoskeleton for stroke and spinal cord injury rehabilitation*”, Rehabilitation Robotics (ICORR), 2011 IEEE International Conference on (pp. 1-5). IEEE.
17. Nef, T., Mihelj, M., Riener, R. (2007), “*ARMin: a robot for patient-cooperative arm therapy*”, Medical & biological engineering & computing, 45(9), 887-900.
18. Carignan, C., Liszka, M. (2005), “*Design of an arm exoskeleton with scapula motion for shoulder rehabilitation*”, Advanced Robotics, 2005. ICAR'05. Proceedings., 12th International Conference on (pp. 524-531). IEEE.
19. Dovat, L., Lamercy, O., Gassert, R., Maeder, T., Milner, T., Leong, T. C., Burdet, E. (2008), “*HandCARE: a cable-actuated rehabilitation system to train hand function after stroke*”, IEEE Transactions on Neural Systems and Rehabilitation Engineering, 16(6), 582-591.
20. Ueki, S., Kawasaki, H., Ito, S., Nishimoto, Y., Abe, M., Aoki, T., Mouri, T. (2012), “*Development of a hand-assist robot with multi-degrees-of-freedom for rehabilitation therapy*”, IEEE/ASME Transactions on Mechatronics, 17(1), 136-146.
21. Krebs, H. I., Volpe, B. T., Williams, D., Celestino, J., Charles, S. K., Lynch, D., Hogan, N. (2007), “*Robot-aided neurorehabilitation: a robot for wrist rehabilitation*”, IEEE Transactions on Neural Systems and Rehabilitation Engineering, 15(3), 327-335.
22. Manna, S. K., Bhaumik, S. (2013), “*A bioinspired 10 DOF wearable powered arm exoskeleton for rehabilitation*”, Journal of Robotics, 2013.
23. Selvi Ö. (2012), “*Structural and kinematic synthesis of overconstrained mechanisms*”, PhD Thesis in Mechanical Engineering, İzmir Institute of Technology (2012)
24. Yılmaz, K. (2016), “*Design of an Overconstrained Manipulator for Rehabilitation Purposes*”, Master Thesis, Çankaya University, 2016
25. Gates, D. H., Walters, L. S., Cowley, J., Wilken, J. M., & Resnik, L. (2016), “*Range of motion requirements for upper-limb activities of daily living*”, American Journal of Occupational Therapy, 70(1), 7001350010, pp 1-10.

26. Nariman-Zadeh N., Felezi M., Jamali A. Ganji M. (2009), "*Pareto optimal synthesis of four-bar mechanisms for path generation*", Mechanism and Machine Theory, 44.1,180-191 (2009)
27. Wen-Yi L. (2010), "*A GA-DE hybrid evolutionary algorithm for path synthesis of four-bar linkage*", Mechanism and Machine Theory, 45.8, 1096-1107 (2010)
28. Acharyya K., Mandal M. (2009), "*Performance of EAs for four-bar linkage synthesis*", Mechanism and Machine Theory, 44.9, 1784-1794 (2009)
29. Hongying Y., Dewei T., Zhixing W (2007), "*Study on a new computer path synthesis method of a four-bar linkage*", Mechanism and machine theory 42.4, 383-392 (2007)
30. Radovan B., Djordjevic R. (2004), "*Optimal synthesis of a four-bar linkage by method of controlled deviation*", Journal of Theoretical and Applied Mechanics, 31.3-4, 265-280 (2004)
31. Huang, T., Li, M., Chetwynd, D. G., Whitehouses, D. J. (2004), "*Optimal Kinematic Design of 2-DOF Parallel Manipulators with Well-Shaped Workspace Bounded by a Specified Conditioning Index*", IEEE Transaction on Robotics and Automation, Vol.20, No.3 pp. 538-543 (2004)
32. Olds, C. (2015), "*Global Indices for Kinematic and Force Transmission Performance in Parallel Robots*", IEEE Transaction on Robotics and Automation, Vol.31, No.2 pp. 494-500 (2015)
33. Dou, R. (2009), "*Optimum design of 3-RRR planar parallel manipulators*", Proc. IMechE Vol.224 Par C: J. Mechanical Engineering Science, pp. 411-418 (2009)
34. Lou, Y. J., Liu, G. F., Li, Z. X. (2005), "*A General Approach for Optimal Design of Parallel Manipulators*", IEEE Transactions on Automation science and engineering, (2005).
35. Stan, S. (2006), "*Workspace optimization of a two degree of freedom mini parallel robot*", Automation, Quality and Testing, Robotics, 2006 IEEE International Conference on Vol. 2, pp. 278-283 (2006)
36. Stan, S. D., Manic, M., Balan, R., Maties, V. (2009), "*Genetic algorithms for workspace optimization of planar medical parallel robot*", IEEE International Conference on Emerging Trends in Computing, ICETIC, pp. 8-10 (2009)
37. Badescu, M., Mavroidis, K. (2004), "*Workspace optimization of 3-legged UPU and UPS parallel platforms with joint constraints*", Journal of Mechanical Design, 126(2), pp. 291-300 (2004)

38. Stock, M., Miller, K. (2003), "*Optimal kinematic design of spatial parallel manipulators: application to linear delta robot*", Journal of Mechanical Design, pp. 292-301 (2003)
39. Gao, Z., Zhang, D. (2011), "*Workspace representation and optimization of a novel parallel mechanism with three-degrees-of-freedom*", Sustainability, pp. 2217-2228 (2011)
40. Zang, H., Zhang, S., Hapeshi, K. (2010), "*A review of nature-inspired algorithms*", Journal of Bionic Engineering, 2010, 7: S232-S237.
41. Yang, X. (2010), "*Nature-inspired metaheuristic algorithms*", Luniver press, 2010.
42. Nedic, N., Prsic, D., Dubonjic, L., Stojanovic, V., Djordjevic, V. (2014), "*Optimal cascade hydraulic control for a parallel robot platform by PSO*", The International Journal of Advanced Manufacturing Technology, 72(5-8), 1085-1098.
43. Saputra, V. B., Ong, S., Nee, A. (2015), "*A swarm optimization approach for solving workspace determination of parallel manipulators*", Robotica, 2015, 33.03: 649-668.
44. ŁUKASIK, S., Żak, S. (2009), "*Firefly algorithm for continuous constrained optimization tasks*", International Conference on Computational Collective Intelligence. Springer Berlin Heidelberg, 2009. p. 97-106.
45. Gosselin, C. M., and Hamel J-F. (1994) "*The agile eye: a high-performance three-degree-of-freedom camera-orienting device.*" Robotics and Automation, 1994. Proceedings., 1994 IEEE International Conference on. IEEE.
46. Fazekas, G., Horvath, M., Troznai, T., Toth, A. (2007) "*Robot-mediated upper limb physiotherapy for patients with spastic hemiparesis: a preliminary study*" Journal of rehabilitation medicine, 39(7), 580-582.
47. Xu, Y., Terekhov, A. V., Latash, M. L., Zatsiorsky, V. M. (2012) "*Forces and moments generated by the human arm: variability and control*" Experimental brain research, 223(2), 159-175.

APPENDIX A: Simmechanics Models of Manipulator

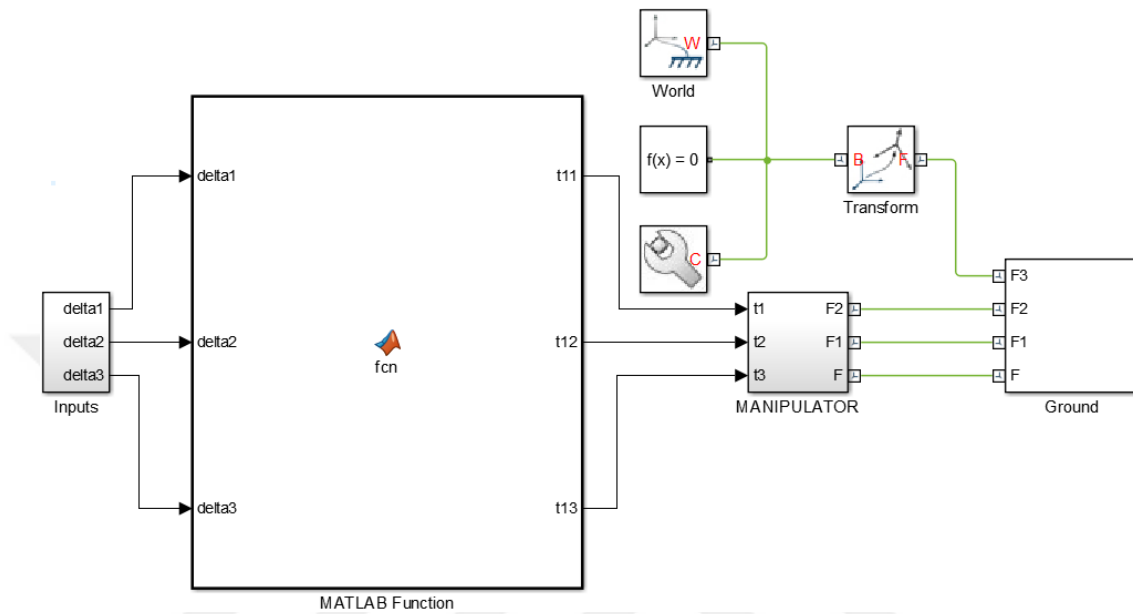


Figure 21. Simmechanics model of spherical part

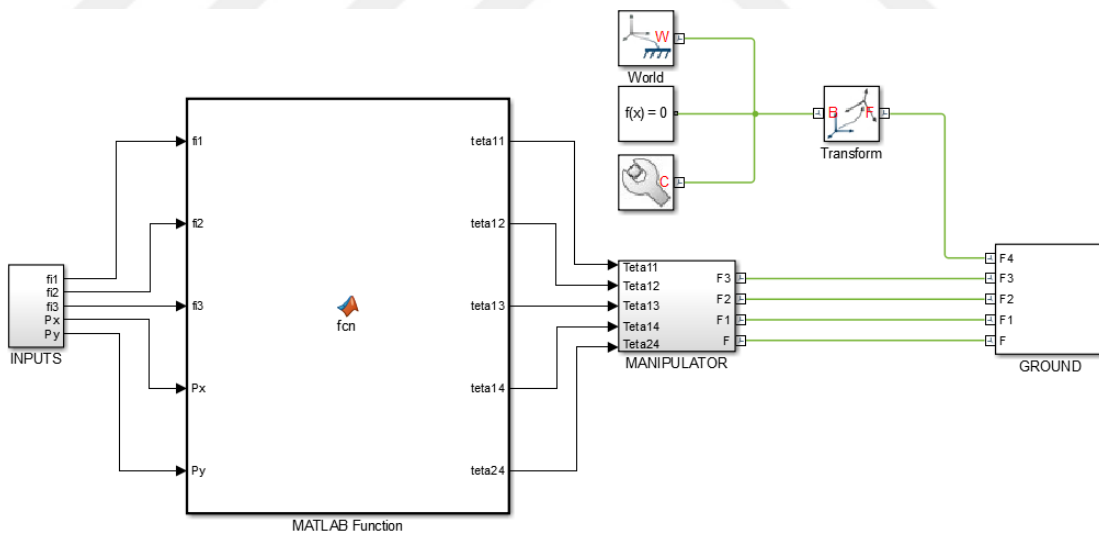


Figure 22. Simmechanics model of planar part

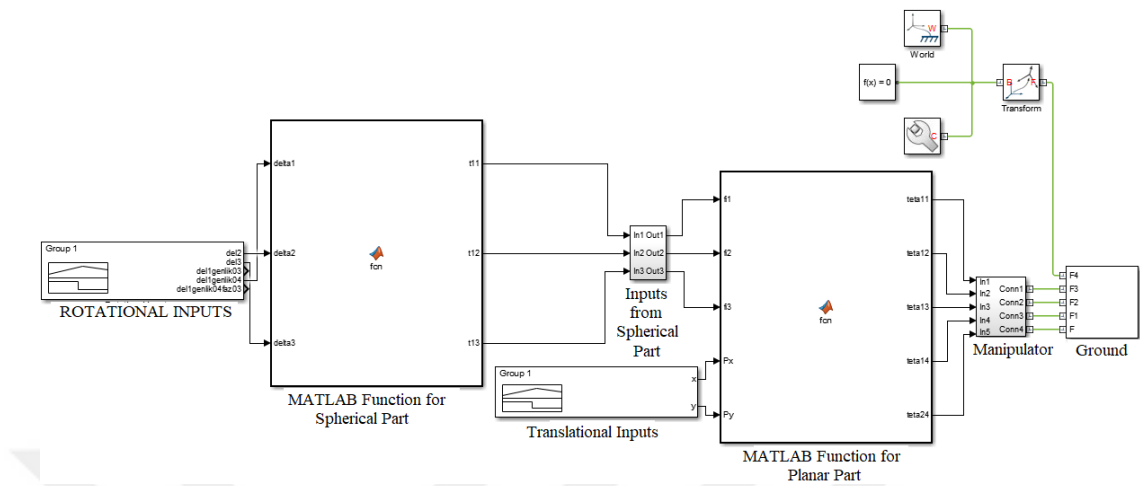


Figure 23. Simmechanics model of whole manipulator

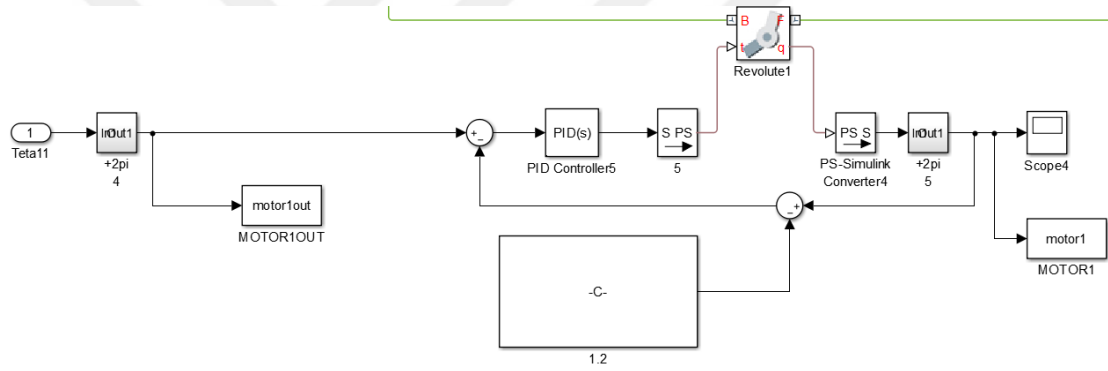


Figure 24. PID control model of any active joint

APPANDIX B: Several Views of Obtained Manipulator

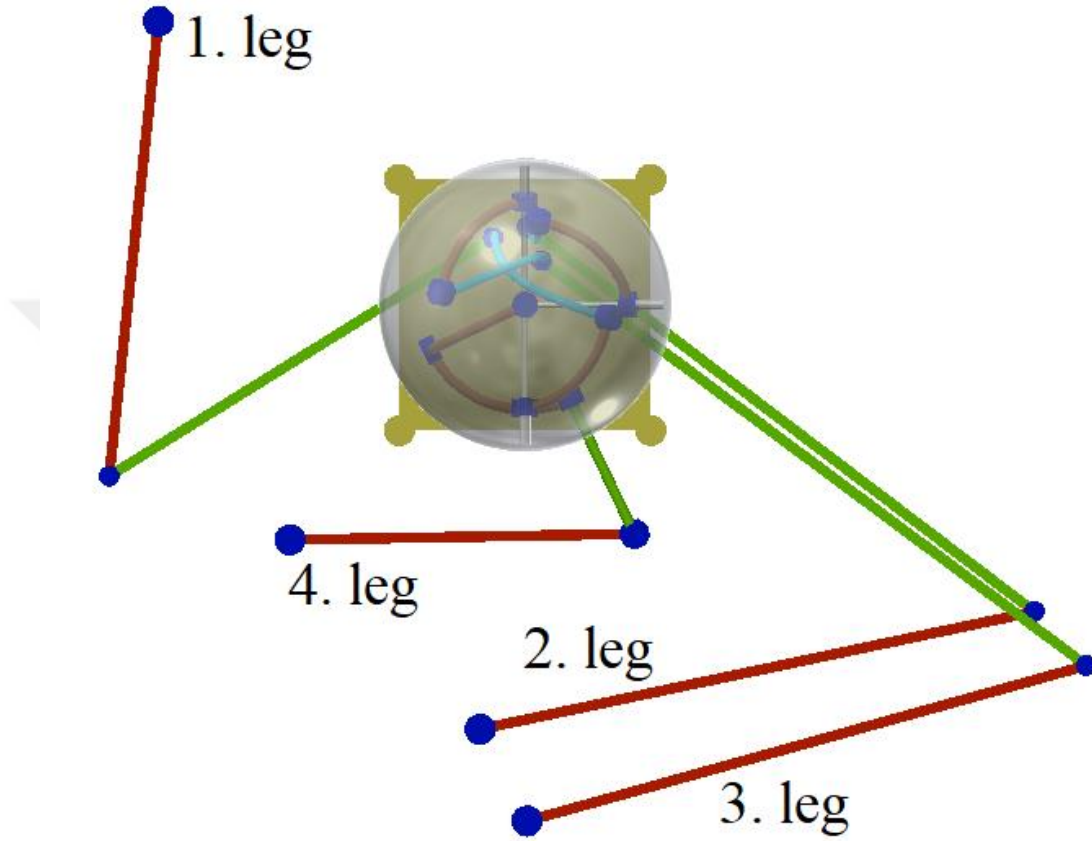


Figure 25. Top view of the manipulator

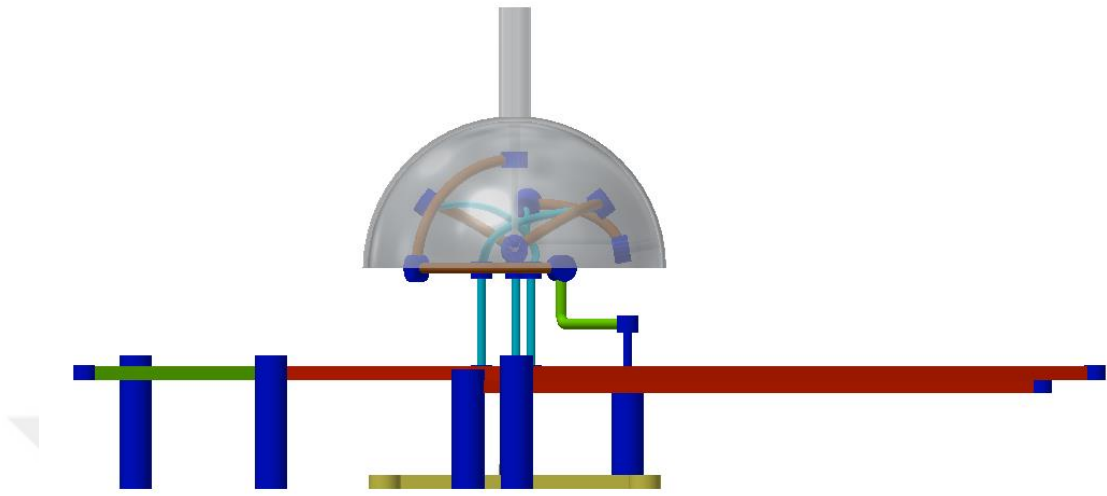


Figure 26. Front view of the manipulator

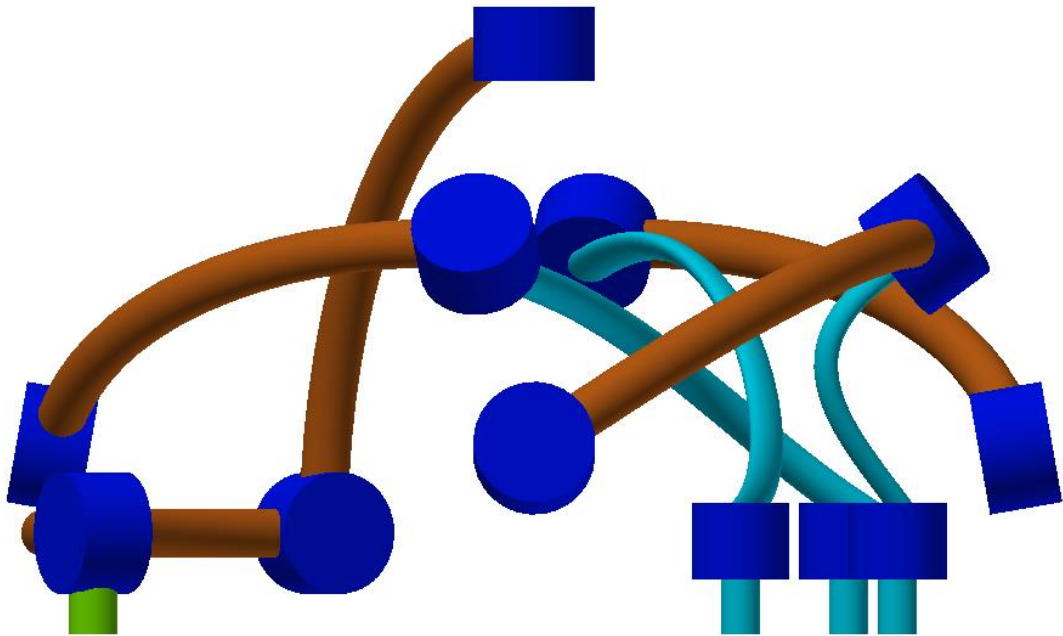


Figure 27. A detailed view of spherical part